

1

2 **Gait signature changes with walking speed are similar  
3 among able-bodied young adults despite persistent  
4 individual-specific differences**

5

6

7 **Taniel S. Winner<sup>1\*</sup>, Michael C. Rosenberg<sup>1</sup>, Gordon J. Berman<sup>2</sup>, Trisha M. Kesar<sup>3</sup>,  
8 Lena H. Ting<sup>1,3</sup>**

9

10 <sup>1</sup> W.H. Coulter Dept. Biomedical Engineering, Emory University and Georgia Institute of  
11 Technology, Atlanta, GA, USA

12 <sup>2</sup> Department of Biology, Emory University, Atlanta, GA USA

13 <sup>3</sup> Department of Rehabilitation Medicine, Division of Physical Therapy, Emory University,  
14 Atlanta, GA, USA

15

16

17

18

19 \* Corresponding author  
20 E-mail: [twinner@emory.edu](mailto:twinner@emory.edu)

21

22

23

24

25

26 **Abstract**

27 Understanding individuals' distinct movement patterns is crucial for health, rehabilitation, and  
28 sports. Recently, we developed a machine learning-based framework to show that "gait  
29 signatures" describing the neuromechanical dynamics governing able-bodied and post-stroke gait  
30 kinematics remain individual-specific across speeds. However, we only evaluated gait signatures  
31 within a limited speed range and number of participants, using only sagittal plane (i.e., 2D) joint  
32 angles. Here we characterized changes in gait signatures across a wide range of speeds, from  
33 very slow (0.3 m/s) to exceptionally fast (above the walk-to-run transition speed) in 17 able-bodied  
34 young adults. We further assessed whether 3D kinematic and/or kinetic (ground reaction forces,  
35 joint moments, and powers) data would improve the discrimination of gait signatures. Our study  
36 showed that gait signatures remained individual-specific across walking speeds: Notably, 3D  
37 kinematic signatures achieved exceptional accuracy (99.8%, confidence interval (CI): 99.1-100%)  
38 in classifying individuals, surpassing both 2D kinematics and 3D kinetics. Moreover, participants  
39 exhibited consistent, predictable linear changes in their gait signatures across the entire speed  
40 range. These changes were associated with participants' preferred walking speeds, balance  
41 ability, cadence, and step length. These findings support gait signatures as a tool to characterize  
42 individual differences in gait and predict speed-induced changes in gait dynamics.

43

## 44 1. Introduction

45 Seemingly stereotypical human behaviors such as walking and running exhibit distinct  
46 individual characteristics<sup>[1-5]</sup> that stem from complex interactions of neural control, muscle  
47 activation patterns, biomechanics, sensory feedback, and the environment. Precisely because of  
48 these interconnected processes, the mechanisms underlying individuality in gait coordination  
49 across speeds remain elusive. Previously, we developed a proof-of-concept framework  
50 leveraging a recurrent neural network (RNN) model to capture individual differences in human  
51 gait dynamics based on measured kinematics<sup>[6]</sup>. The high-dimensional internal parameters of the  
52 trained model encode how individuals' inter- and intra-limb gait variables progress over time. From  
53 the model's internal activations, we constructed low-dimensional representations of individuals'  
54 multi-joint coordination, phase-averaged across multiple strides, termed *gait signatures*. Gait  
55 signatures have broadened our understanding of human inter-joint coordination, going beyond  
56 traditional analyses focused on discrete spatiotemporal<sup>[7]</sup>, kinematics and kinetics<sup>[8]</sup>, and other  
57 derived metrics of gait coordination<sup>[9-13]</sup>. Thus, our prior work introduced a method that showed  
58 promise using 2D joint angles to identify individual differences in gait signatures that remain  
59 individual-specific across a restricted range of walking speeds in both able-bodied and impaired  
60 gait<sup>[6]</sup>. Here, we tested the ability of gait signatures, derived from different data types (3D  
61 kinematics and 3D kinetics), to discriminate individuals amidst a wide range of speeds.  
62 Additionally, we examined gait signatures in able-bodied young adults across a wide range of  
63 walking speeds to understand their speed-dependent variations. Finally, to uncover potential  
64 factors influencing speed-dependent modifications in gait signatures, we investigated whether  
65 these changes correlate with specific spatiotemporal variables and dynamic balance.

66 We hypothesize that individual differences in gait dynamics persist across a wide range  
67 of walking speeds. This persistence allows us to identify individuals by their gait signatures  
68 regardless of gait speed, despite the biomechanical changes required to walk at different speeds.  
69 To modulate gait speed from slow to a faster pace, individuals can employ various strategies,  
70 including taking longer steps, increasing step frequency, and decreasing the swing or stance  
71 phase durations, among others<sup>[14-17]</sup>. Increasing gait speed has also been associated with  
72 complex changes in joint excursions and step length asymmetry in people post-stroke<sup>[18,19]</sup>.  
73 However, previous research demonstrated that speed had little effect on joint-level coordination  
74 in injury-free adults<sup>[20,21]</sup>. Building on our previous findings<sup>[6]</sup>, where we demonstrated discernible  
75 individual gait signatures across a limited range of speeds, we anticipate that although gait  
76 signatures would change across a wider speed range, their individual-specific nature would be  
77 preserved.

78 Understanding what data are needed to differentiate gait coordination patterns between  
79 individuals may inform experimental design, equipment considerations, and future clinical  
80 translation. Our prior work<sup>[6]</sup> constructed gait signatures using only sagittal-plane joint kinematics  
81 (i.e. joint angles). However, including additional kinematic and kinetic (i.e. ground reaction forces,  
82 joint moments, and powers) data may offer further insights into the individual-specificity of gait  
83 signatures. While majority of gait variability occurs in the sagittal plane, variability may also  
84 manifest in the frontal and coronal planes among certain able-bodied individuals, evident in  
85 movements like hip abduction/adduction and internal rotation<sup>[22]</sup>. This variability becomes more  
86 pronounced in impaired individuals, such as stroke survivors, who often adopt compensatory  
87 strategies in the frontal plane, like circumduction or pelvic hiking<sup>[23-25]</sup>. Furthermore, kinetic  
88 information may be important to include as kinetics might contain meaningful information not

89 encoded in the kinematics<sup>[25]</sup>. For example, two people with identical kinematics and different  
90 body compositions will have different kinetics<sup>[26]</sup>. Alternatively, estimated joint kinematics and  
91 kinetics are mechanically related, such that kinetics may not be necessary to distinguish  
92 individuals if soft-tissue artifacts and measurement errors<sup>[27]</sup> are negligible, compared to individual  
93 differences in kinematics<sup>[28-30]</sup>.

94 Given similar biomechanical constraints and unimpaired neural control in able-bodied  
95 young adults, we hypothesize that there exist common changes in gait dynamics across speeds.  
96 Numerous studies have reported many discrete gait parameters that increase with gait speed,  
97 including leg stiffness<sup>[31]</sup>, center-of-mass work and power<sup>[32]</sup>, muscle activity amplitude<sup>[33]</sup>, joint  
98 angle excursions<sup>[34]</sup>, kinetic variables<sup>[20,35]</sup>, and spatiotemporal variables<sup>[14,16,17,36,37]</sup>. Moreover,  
99 previous research has identified many relationships between specific gait characteristics and  
100 walking speed<sup>[32]</sup>. For example, spatiotemporal parameters demonstrate squared and cubic  
101 relationships, while kinematic outcomes exhibit a range of linear, squared and cubic relationships  
102 with normalized gait speed<sup>[38]</sup>. Additionally, certain kinetic parameters exhibit a linear relationship  
103 with gait speed, while others display quadratic relationships<sup>[39]</sup>. While common measures of gait  
104 biomechanics exhibit differential relationships with speed, we tested whether gait signatures  
105 would also exhibit a consistent relationship with speed. As gait signatures leverage continuous,  
106 synchronously measured gait data to identify a low-dimensional representation of gait dynamics,  
107 they may provide a more comprehensive representation of how gait coordination changes with  
108 speed. This approach may shed light on the underlying organization of gait variables, enriching  
109 our understanding of how gait dynamics change across speeds.

110 Understanding whether changes in gait signatures across different speeds correlate with  
111 changes in discrete spatiotemporal variables and dynamic balance ability would highlight potential  
112 factors impacting how people modulate coordination across speeds. Studies show that walking  
113 at extremely slow speeds disrupts individuals' natural momentum and coordination<sup>[40]</sup> and  
114 biomechanical strategies<sup>[41]</sup>. We hypothesize that an individual's capacity to modulate their gait  
115 with speed is contingent upon underlying factors inherent to their sensorimotor system and  
116 functional capacity. We predict that individuals with better balance ability may be able to adapt  
117 more flexibly (exhibit less change in their signature) to walking at extremely slow or fast treadmill  
118 speeds than those with lower balance ability.

119 This study assesses whether able-bodied young adults' gait signature remain individual-  
120 specific walking speeds ranging from extremely slow (0.3m/s) to exceptionally fast (above the  
121 empirical walk-to-run transition). First, we determined the optimal number of speed trials per  
122 individual required to train a linear support vector machine classifier effectively, enabling  
123 accurate individual identification across various speeds for each data type. Next, we characterized  
124 how the data type used to train the gait signatures model (2D kinematics, 3D kinematics, 3D  
125 kinetics and their combination) impacted the ability to identify individuals based on their gait  
126 signatures using a support vector machine classification task. Thirdly, we characterized the extent  
127 to which individuals exhibited consistent changes in gait signatures with speed. Lastly, we  
128 determined whether changes in gait signatures with speed were associated with changes  
129 biomechanical variables and individuals' dynamic balance ability.

130 **2. Materials and methods**

131 **2.1 Ethics statement**

132 All participants provided written informed consent prior to study participation, and the study  
133 protocol was approved by the Emory University Institutional Review Board.

134 **2.2 Human subject participants**

135 Seventeen young able-bodied adult individuals participated in this study (8 men, 9 women);  
136 mean  $\pm$  s.d. age =  $27.9 \pm 4.5$  years, height =  $1.7 \pm 0.1$  m, body mass =  $77.0 \pm 21.8$  kg).  
137 Participants reported no history of injury or pain in the last 3 months.

138 **2.3 Experimental design**

139 To test the effect of a wide range of speeds, participants completed 60-second trials at 9 different  
140 speeds ranging from extremely slow to extremely fast speeds. The speed conditions were  
141 implemented in 2 phases, and within each phase speeds were assessed in random order. Phase  
142 1 was always implemented first and consisted of 6 speed conditions ranging from the fixed  
143 extreme slow speed of 0.3 m/s to each participant's fastest comfortable safe speed determined  
144 on the treadmill. Phase 2 was implemented second and consisted of the 3 remaining speed  
145 conditions (92.5%, 100.0%, and 107.5% of the empirical walk-to-run transition speed).  
146 Participants were advised to take a seated or standing rest break for 1-2 minutes as needed, and  
147 if they experienced fatigue or pain following a gait trial. The 9 speeds evaluated for each  
148 participant are outlined below as follows:

149 ***Phase 1 speed conditions***

- 150 1. Fixed extreme slow: a very slow fixed speed of 0.3 m/s was selected to match the speed  
151 of low functioning stroke survivors.
- 153 2. Slow overground-derived: participants were instructed to walk at a very slow pace  
154 overground (instruction: "walk as if leisurely strolling in a beautiful park") along a flat, indoor  
155 marked 29.9-foot (9.11-meter) path in a controlled lab setting. Three trials were performed  
156 and the average speed for this condition was calculated for each participant.
- 158 3. Self-selected treadmill-derived: The treadmill was initiated at ~1 m/s and participants were  
159 instructed to indicate whether to increase or decrease the speed until they reached a  
160 speed that was representative of their natural or comfortable walking speed.
- 162 4. Self-selected overground-derived: participants were instructed to walk at their natural self-  
163 selected pace overground (instruction: "walk at a pace that is natural for you to travel from  
164 point A to B") along a flat, smooth, marked 29.9-foot path in a controlled lab setting. Speed  
165 was determined as the average speed from three trials.
- 167 5. Intermediate calculated: The speed halfway in between each participant's self-selected  
168 overground-derived and the fast treadmill-derived speed was calculated.
- 170 6. Fast treadmill-derived: The treadmill was initiated at ~1 m/s and participants were  
171 instructed to indicate whether to increase or decrease the speed until they reached a  
172 speed that was representative of a fast-walking speed (instruction: "walk as if you are  
173 running late for a very important event").

174

## Phase 2 speed conditions

175

- 176 7. 92.5% of the walk-to-run transition speed: 7.5% below the determined walk-to-run  
177 transition speed was calculated.
- 178 8. Walk-to-run transition speed: The walk-to-run transition speed was determined before  
179 randomizing the 3 speed conditions in phase 2. The treadmill was initiated around each  
180 individuals' determined fast walking speed, and participants were instructed to indicate  
181 whether to increase or decrease the speed until they reached a speed that felt they could  
182 no longer walk and needed to start running. Treadmill speeds were varied by 0.05m/s -  
183 0.13m/s at a time. Once participants identified a preferred transition speed, the treadmill  
184 speed was increased beyond, then decreased below, that speed to encourage exploration  
185 of each speed. Participants were instructed to try walking and running at each speed (~20  
186 seconds), if possible. Next, participants were again asked to identify the speed beyond  
187 which they prefer to run and below which they prefer to walk. This process was repeated  
188 until participants selected two consecutive speeds within 0.05 m/s of each other. The  
189 recorded speed was the one they settled on during the process. This approach is similar  
190 to another study<sup>[42]</sup> however, we did not mandate rest periods.
- 191 9. 107.5% of the walk-to-run transition speed: 7.5% above the determined walk-to-run  
192 transition speed was calculated.

193

194

195

## 2.4 Data acquisition and processing

196

197

198

199

200

201

202

203

204

205

206

207

We used 3D motion capture to obtain continuous walking data from participants. Reflective markers were attached to participants' trunk, pelvis, and bilateral shank, thigh, and foot segments<sup>[43]</sup>. We collected marker position data while participants walked on a split-belt instrumented treadmill (Bertec Corp., Ohio, USA) using a 7-camera motion analysis system (Vicon Motion Systems, Ltd., UK). Marker data were collected at 100Hz, and synchronous ground reaction forces were recorded at 2000 Hz and were down sampled to 100Hz using previously established techniques<sup>[43-46]</sup>. Raw marker position data were labeled and gap-filled. Marker trajectories and ground reaction force raw analog data were low-pass filtered at 6 and 30 Hz in Visual 3D (C-Motion Inc., Maryland, USA). Gait events (bilateral heel contact and toe-off) were determined using a 20N vertical GRF cutoff; 3D kinematics and kinetics were calculated in Visual 3D.

208

209

210

211

212

213

214

215

216

217

218

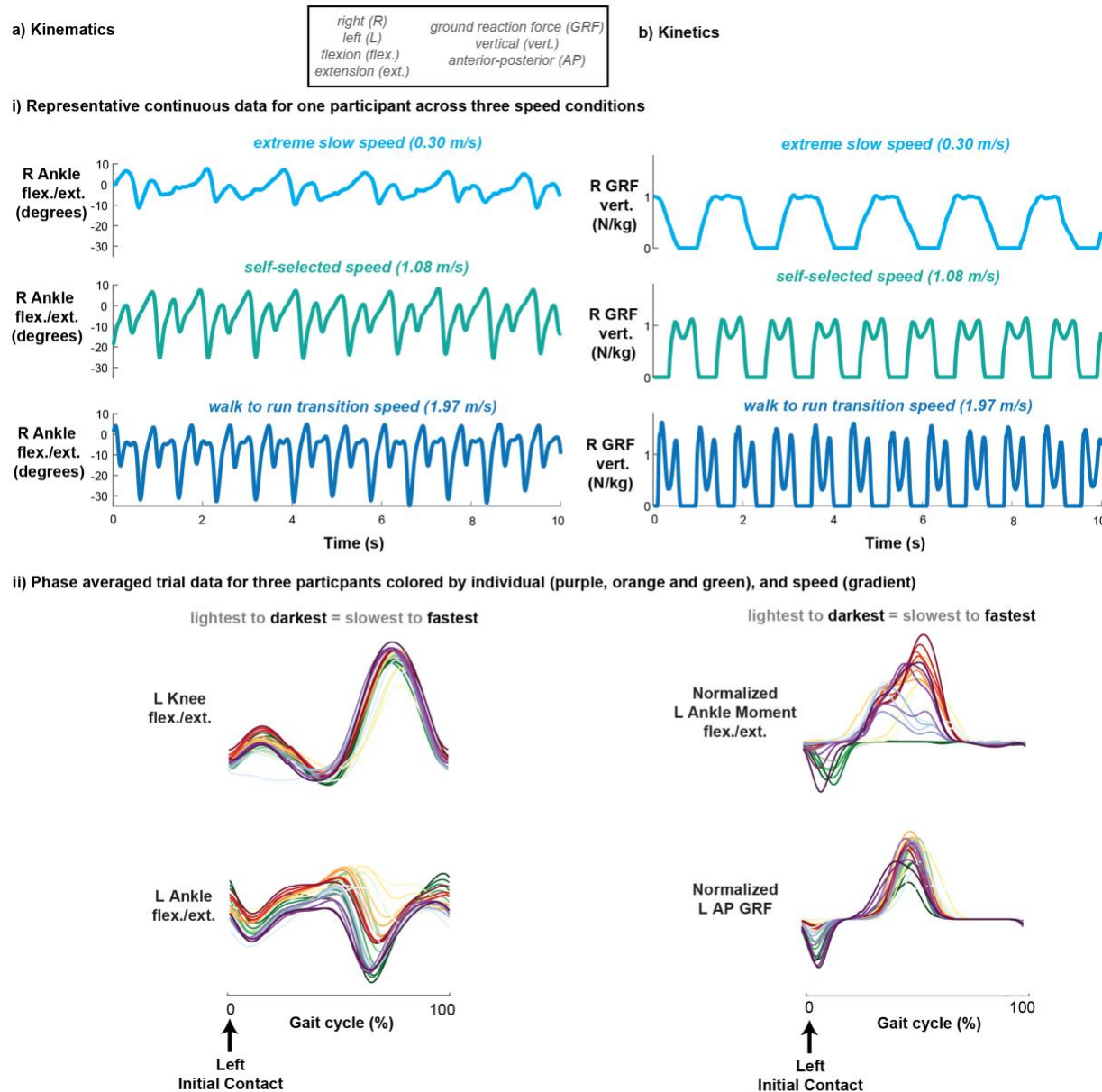
219

220

To describe the 3D kinematics of each individual, we measured 18 continuous variables from the motion capture data; bilateral hip, knee, and ankle joint angles each in the sagittal, frontal, and transverse planes. Two-dimensional kinematics consisted of 6 continuous features, comprising bilateral hip, knee, and ankle joint angles in the sagittal plane only. 3D kinetics consisted of 42 total features- bilateral ground reaction forces normalized to body weight, ankle, knee and hip moments and powers each in the sagittal, frontal, and transverse planes. A combination of all the data consisted of 60 variables. sagittal-plane hip, knee, and ankle joint kinematics. Three speed trials were omitted (2 for participant YA04 and 1 for participant YA06) due to technical errors during data collection, resulting in a reduction of the full trial data set from N = 153 to N = 150. The excluded trials corresponded to YA04 and YA06's 7.5% below walk-to-run transition speed, and YA4's 7.5% above walk-to-run transition speed. To visualize representative traces of 3D kinematics and kinetics across different speeds, refer to (Fig. 1). One minute of continuous 3D motion capture treadmill walking data were collected from 17 able-bodied

221 young adults across 9 different speed conditions (Fig. 2a). Continuous gait data from all  
222 individuals and speed conditions were extracted (Fig. 2b).

223



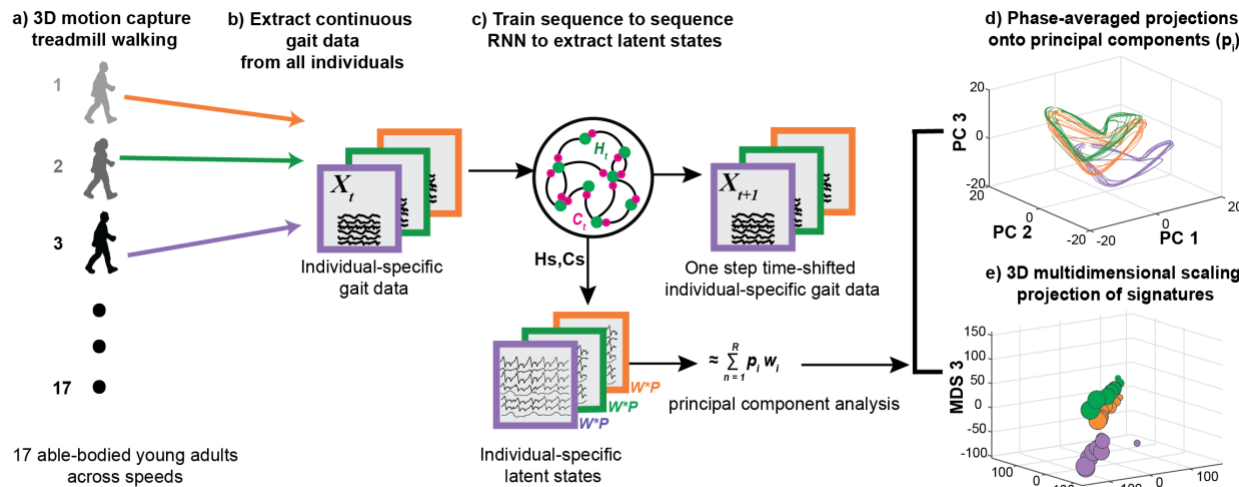
224

225 **Figure 1: Visualization of representative a) kinematic and b) kinetic treadmill walking data.**  
226 **Representative continuous right angle flexion/extension (a-i) and right vertical ground**  
227 **reaction force (b-i) for one participant across three speed conditions: extreme slow,**  
228 **self-selected, and extreme fast (walk to run transition). Representative phase-averaged left**  
229 **knee flexion/extension (a-ii, top), left ankle flexion/extension (a-ii, bottom), normalized left**  
230 **ankle moment flexion/extension (b-ii, top), and normalized left anterior-posterior ground**  
231 **reaction force (b-ii, bottom) data for three participants colored by individual (color) and**  
232 **speed (gradient).**

## 233 2.5 Generating gait signatures

234 To create gait signatures, we utilized the RNN framework described previously<sup>[6]</sup>, where  
235 continuous, multi-joint kinematics from multiple individuals and speeds were used to train an RNN  
236 model. The RNN model architecture consisted of a single input layer, a hidden layer with 512 long  
237 short-term memory (LSTM) activation units, and an output layer. The model was trained using an  
238 Adam optimizer<sup>[47]</sup> in a sequence-to-sequence manner to predict one-step time shifted output  
239 kinematics (Fig. 2c). To prevent overfitting on this larger dataset of stereotypical able-bodied gait  
240 patterns, we made the following modifications to our prior framework<sup>[6]</sup>. We lowered the learning  
241 rate of the Adam optimizer from 0.001 in to 0.0001, added a drop out layer after the hidden layer  
242 with 20% drop out rate, and added a kernel L2 regularization (regularization strength of 0.01).  
243 Additionally, the trials in this able-bodied young adult dataset were 60 seconds long vs. the 15  
244 second trials used previously. During training, our data were batched according to the number of  
245 total trials (N = 150). and the RNN was trained on all individuals trials to extract individual-specific  
246 latent states of the RNN which represent individuals' gait dynamics (Fig. 2c, Individual-specific  
247 latent states).

248 The RNN latent states (Fig. 2c, Individual-specific latent states), were extracted for all  
249 individuals' trials, reduced in dimension using and principal component analysis and phase-  
250 averaged<sup>[48]</sup> to generate gait signatures. Gait signatures can be visualized as looped  
251 representations of specified principal component (PC) projections (Fig. 2d) and 3D multi-  
252 dimensional scaling projections (Fig. 2e). We trained four individual RNN models, each with a  
253 different input data type (2D kinematics, 3D kinematics, 3D kinetics and a combination of the  
254 data). Gait signatures were generated for each model RNN model separately.



255  
256 **Figure 2: Pipeline of the gait signatures framework and outcomes. a) 3D motion capture**  
257 **data from 17 able-bodied young adults walking on a treadmill across 9 speeds each was**  
258 **conducted. b) Continuous timeseries kinematics and kinetics were extracted from all trials.**  
259 **c) A sequence-to-sequence RNN was trained using subsets of the data recorded in (b), and**  
260 **individual-specific gait signatures were extracted for all individuals' trials. d) Principal**  
261 **component analysis was applied to reduce the dimensionality of the high dimensional**  
262 **latent states, each trial was phase-averaged, and the first 3 dominant PCs visualized as 3D**  
263 **loops. e) 3D projections of low-dimensional gait signatures using multidimensional scaling**

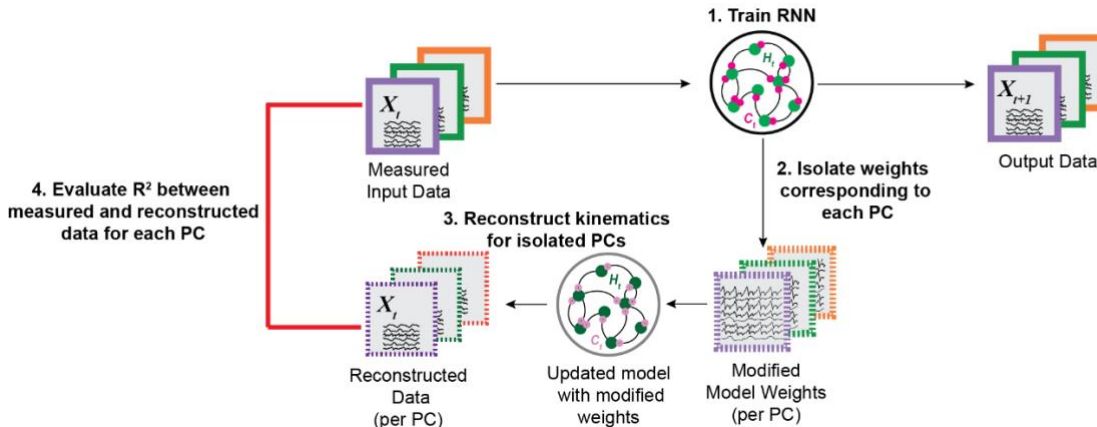
264 **reveal individual-specific gait signatures among 3 representative able-bodied young**  
265 **adults.**

266 **2.6 Determining the variance explained in the original features by the principal**  
267 **components of the gait signatures model**

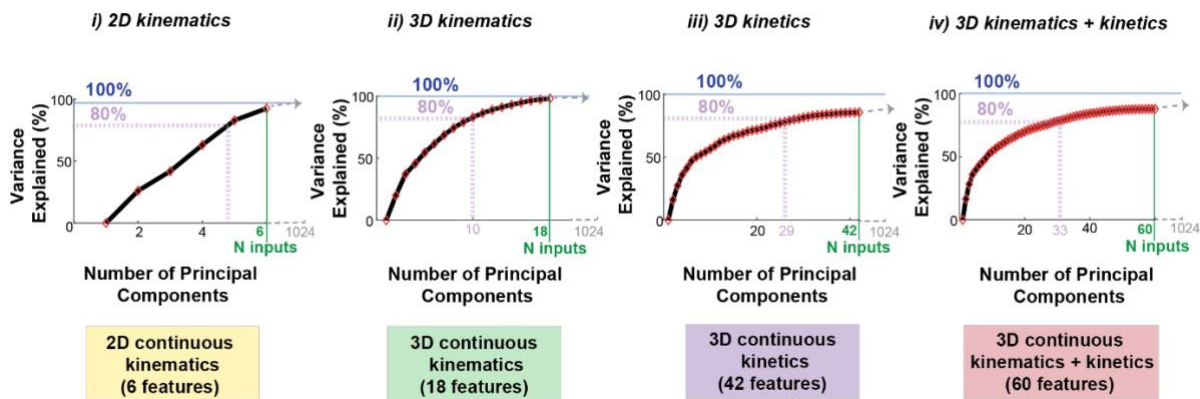
268 To attain the variance explained in the original features by each principal component (PC)  
269 of the RNN latent spaces, we used each trained RNN model (Fig. 3a, 1. Train RNN), extracted  
270 the model internal activations (weights), performed PCA on them, and identified the weights  
271 corresponding to each PC (Fig. 3a, 2. Isolate weights corresponding to each PC). The model  
272 weights were updated to a new model based on the top N principal components and used to  
273 generate reconstructed data for the provided internal states (Fig. 3a, 3. Reconstruct data for  
274 isolated PCs). The coefficient of determination ( $R^2$ ) was calculated between the reconstructed  
275 data and the measured data (Fig. 3a, 4. Evaluate the  $R^2$  between measured and reconstructed  
276 data for each PC). Eigenvalue plots of the cumulative variance explained by each PC of the gait  
277 signature (expressed as a percentage) were constructed for each data type (Fig. 3b).

278 To determine the number of principal components to retain, the elbow of the eigenvalue  
279 plot is usually considered sufficient<sup>[49]</sup>. However, since our eigenvalue plots represent the variance  
280 explained by PCs of the original data (not of the high-dimensional gait signatures i.e., internal  
281 activations), we determined a reasonable threshold of 80% to account for most of the variance  
282 explained in the original model input data.

a) Determination of the variance explained in the original signals by the principal components (PCs) of the gait signature model



b) Eigenvalue plots of variance explained by each principal component of the gait signature across the four signals



283

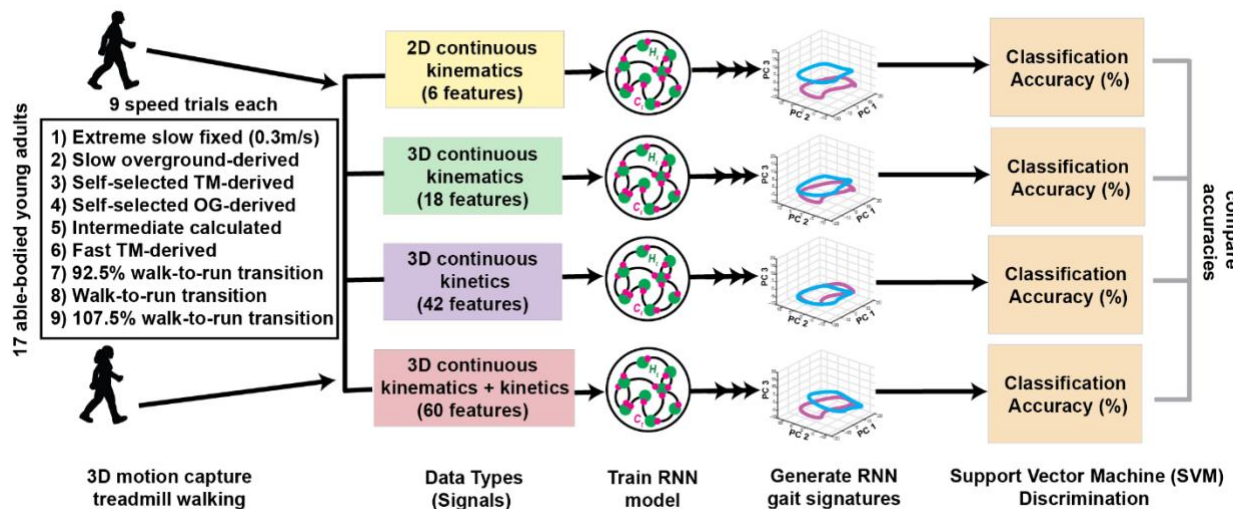
284 **Figure 3: Variance explained in the original signals by each of the principal components**  
285 **of the extracted dynamics. a) To determine the variance explained in the original data by**  
286 **the dynamics: 1) the RNN model was trained, 2) the trained model weights (internal**  
287 **activations) were extracted and the dynamics corresponding to each PC was isolated. 3)**  
288 **For each PC, the original signals were reconstructed across participants. 4) The coefficient**  
289 **of determination was calculated between the measured input signals and the**  
290 **reconstructed signals for each PC. These values were used to construct eigenvalue plots**  
291 **for each signal type. b) Eigenvalue plots of the cumulative variance explained by**  
292 **increasing number of principal components of the gait signature for each of the four signal**  
293 **types.**

294 **2.7 Discriminating individuals and speeds**

295 To determine whether gait signatures remain characteristic to an individual across a wide range  
296 of walking speeds, we used a linear support vector machine (SVM) discrimination classification  
297 task to classify individuals based on their gait signatures across their nine speed trial conditions.  
298 To maintain consistency in the number of trials per participant analyzed, individuals with fewer  
299 than nine speed trials were excluded from this analysis. The resultant dataset comprised 14  
300 individuals, each with nine different speed condition trials. For each data type, eight distinct  
301 SVM classifiers were trained on a progressive selection of one to eight random trials per

302 individual over 140 total runs using built in MATLAB function 'templateSVM' with standardized  
303 features. The random number generator seed was set to the run number on each iteration for  
304 consistency across the different models. The average classification accuracy across the runs  
305 corresponding to the number of speed trials per individual in the training set was calculated for  
306 each data type. We conducted this analysis separately for the gait signatures across data types  
307 (Fig. 4, **Discrimination task**).

308 Because our gait signature classification accuracies do not obey gaussian statistics, we  
309 used non-parametric Mann-Whitney U tests to test for differences in classification accuracy  
310 between gait signatures generated from 2D versus 3D inputs. For classifiers trained using one to  
311 eight speed trials per participant, we compared classification accuracy and reported p-values and  
312 Mann-Whitney U effect sizes ( $r$ ). An effect size ( $r$ ) smaller than 0.3 indicates a small effect, a value  
313 between 0.3 and 0.5 suggests a medium effect, while an effect size greater than 0.5 indicates a  
314 large effect.



315  
316 **Figure 4: Schematic outlining the comparison of individual discriminatory power between**  
317 **the gait signatures generated using four different signals (2D kinematic, 3D**  
318 **kinematic and a combination of all signals). 3D motion capture of treadmill walking was**  
319 **obtained from 17 able-bodied young adults, encompassing 9 different speed conditions.**  
320 **The four data types were created, each with varying number of features. RNN models were**  
321 **trained for each data type and respective gait signatures were generated. The**  
322 **classification accuracy of individuals across different speeds was assessed using support**  
323 **vector machine (SVM) classifiers, and the classification accuracies between the four gait**  
324 **signature types were compared.**

325 To assess the individual discriminatory potential of discrete biomechanical variables  
326 across speeds, we conducted a comparable SVM classification approach. Specifically, we  
327 focused on 26 widely recognized bilateral kinematic and kinetic discrete variables commonly used  
328 in gait analyses<sup>[6]</sup>, as detailed in [Supplementary Table T1](#). Additionally, we explored the  
329 discriminatory capacity of only the 18 kinematic-only and eight kinetic-only variables in  
330 distinguishing individuals.

332 **2.8 3-D Multi-dimensional scaling map to compare gait signatures**

333 To analyze and visualize the pairwise distances between gait signatures, we employed  
334 multi-dimensional scaling (MDS) to project all gait signatures onto a single 3D gait map. This  
335 technique was used to lower the dimension of our complex high-dimensional signatures,  
336 maximally preserving relationships between individuals and trials.

337 To quantify the intra- vs. inter-individual differences in 3D MDS signatures, the Euclidean  
338 distances were calculated between all signatures within an individual and between individuals,  
339 respectively. Subsequently, a histogram of the Z-scored Euclidean distances was plotted to  
340 visualize both intra and inter- individual distances and the Mann-Whitney U test was performed  
341 on the distributions of distances.

342 **2.9 Identifying relationships between gait signatures and speed**

343 To determine if the relationship between 3D MDS coordinates and gait speed is linear,  
344 simple linear regression was performed separately for each of the three MDS coordinates and  
345 the speed for each individual. Box plots illustrating the slope and  $R^2$  values of the linear fits were  
346 generated, and the mean and 95% confidence intervals of these distributions were recorded.  
347 Additionally, p-values were recorded for the linear fits of each participant.

348 To test whether individuals exhibit similar linear changes in dynamics across speeds, we  
349 used linear mixed effects (LME) models to predict each trial's 3D MDS coordinates from speed  
350 trials. We estimated positions in 3D MDS, separately for each dimension, using linear mixed-  
351 effects models with fixed intercepts and effects of speed, and a random intercept for subject. The  
352 fixed and random effects coefficients differ in each dimension. The models assume that the  
353 relationship between MDS location and trial speed is linear, while allowing for individual  
354 differences in the mean location of gait signatures in MDS space. The models aim to capture how  
355 the overall changes in gait signatures correspond to changes in speed for different subjects. MDS  
356 3D coordinates (X, Y and Z) are the dependent variables (to be predicted), trial speed is the  
357 predictor variables and individuals' Subject ID was used as a categorical random intercept  
358 (Equation 1).

359

$$360 \begin{bmatrix} MDS_X \\ MDS_Y \\ MDS_Z \end{bmatrix} \sim \begin{bmatrix} \beta_{0,X} \\ \beta_{0,Y} \\ \beta_{0,Z} \end{bmatrix} + \begin{bmatrix} \beta_{1,X} \\ \beta_{1,Y} \\ \beta_{1,Z} \end{bmatrix} * speed + \begin{bmatrix} (1|Subject)_X \\ (1|Subject)_Y \\ (1|Subject)_Z \end{bmatrix} \quad (1)$$

361

362 We performed a hierarchical bootstrapping analysis<sup>[50]</sup> to examine how sensitive the model  
363 parameters are to variations in the input data, the number of trials chosen per individual, and the  
364 speed trials used in training. Specifically, we conducted 17 leave-one-subject-out LME models to  
365 predict 3D MDS coordinate positions from gait speed. We manipulated the number of speed trials  
366 chosen per subject (ranging from four to eight) across five iterations, with five random selections  
367 of speed trials per trial count.

368

369

370 **2.10 Relationships between gait signatures and individual differences in mobility**  
371 **to walking speed and changes in gait signatures**

372 To determine whether changes in gait signatures with speed are associated with  
373 individual's functional abilities, we used a narrowing beam balance test, which has been used to  
374 characterize walking balance and motor coordination<sup>[51]</sup>. The narrowing beam balance score,  
375 representing the distance travelled in feet travelled along the narrowing beam, was calculated as  
376 the average distance across four trials. We used linear regression and assessed the correlation  
377 coefficient (Pearson's r) between balance score and the following variables: a) self-selected  
378 walking speed, b) Euclidean distance between SS and extreme slow signatures and c) Euclidean  
379 distance between SS and extreme fast signatures. Additionally, to assess whether SS walking  
380 speed are associated with the extent to which participants altered their gait signatures, we  
381 performed linear regression between the Euclidean distance between SS and extreme slow  
382 signatures vs. SS speed.

383 **2.11 Exploratory analysis of gait signatures and spatiotemporal variables**

384 To determine whether changes in gait signatures with speed reflected similar findings in  
385 the literature about changes in spatiotemporal variables with speed, we conducted an exploratory  
386 analysis to determine whether changes in gait signatures (Euclidean distance) between both self-  
387 selected (SS) and extreme slow, and extreme fast speeds were associated with discrete, trial-  
388 averaged spatiotemporal biomechanical variables. Ten different Pearson's r correlation tests  
389 were conducted for bilateral biomechanical variables: cadence, stance duration, swing duration,  
390 step width, and step length. The alpha value of 0.05 was corrected using Bonferroni method<sup>[52]</sup>  
391 for the 10 different tests per speed modulation type (SS to extreme slow and SS to extreme fast)  
392 and updated to 0.005 each.

393 **3. Results**

394 In summary, individual differences in gait signatures were maintained across the full range of  
395 walking speeds from extremely slow to the walk to run transition. 3D kinematic gait signatures  
396 achieved almost perfect individual classification accuracy of 99% (CI: 99.1-100%), using four or  
397 more random speed trials in the SVM classifier training set. While individual classification  
398 performance was also relatively high for 2D kinematics (95.0%, CI: 88.1-100%) and 3D kinetics  
399 (97.8%, CI: 99.7-98.8%), it remained lower compared to that of 3D kinematic gait signatures.  
400 Linear mixed effects models revealed that individuals exhibited similar changes in their gait  
401 signatures across different speeds. This analysis uncovered a unifying framework for the impact  
402 of speed on gait signatures. We found a significant positive correlation between changes between  
403 SS and the extreme slow speed gait signatures and an external measure of balance ability ( $p =$   
404 0.01,  $r = 0.60$ ). Furthermore, an exploratory analysis revealed that changes between SS and  
405 extreme slow signatures show significant, positive, linear relationships with speed-induced  
406 changes in two out of five spatiotemporal variables: cadence and step length.  
407

408 **3.1 Kinematics and kinetics during treadmill walking differ qualitatively across**  
409 **individuals and speeds**

410 Representative right sagittal plane ankle kinematics (Fig. 1a-i) and right vertical ground  
411 reaction forces (Fig. 1b-i) were relatively consistent across all strides within an individual's trial.

412 Slower-speed trials resulted in fewer gait cycles than faster-speed trials over the shown 10-  
413 second period with noticeable larger joint excursions and ground reaction forces with increasing  
414 speed (Fig. 1ab-i). Despite similar general shapes of phase-averaged kinematics and kinetics  
415 across participants and speeds, there was evident nuanced variability (Fig. 1ab-ii).

416 **3.2 Kinematic gait signatures demonstrate low dimensionality, contrary to kinetic  
417 gait signatures**

418 All gait signature data types met the criterion of explaining at least 80% variance in the  
419 original data signals while using fewer than 34 PCs. However, the number of PCs required to  
420 achieve this threshold varied among different gait signature types (Fig. 3b). Specifically, six PCs  
421 of 2D kinematic signatures capture over 90% of the variance in the original sagittal plane  
422 kinematics (Fig. 3b-i). On the other hand, 3D kinematic gait signatures require 10 principal  
423 components to account for ~83% of the variance in the original features (Fig. 3b-ii). Notably, in  
424 3D kinetic signatures and combined kinematic and kinetic signatures, achieving at least 80%  
425 variance necessitated 29 and 33 PCs respectively (Fig. 3b-iii and iv).

426  
427 **3.3 Kinematic data types preserve individual differences in gait signatures across  
428 speeds**

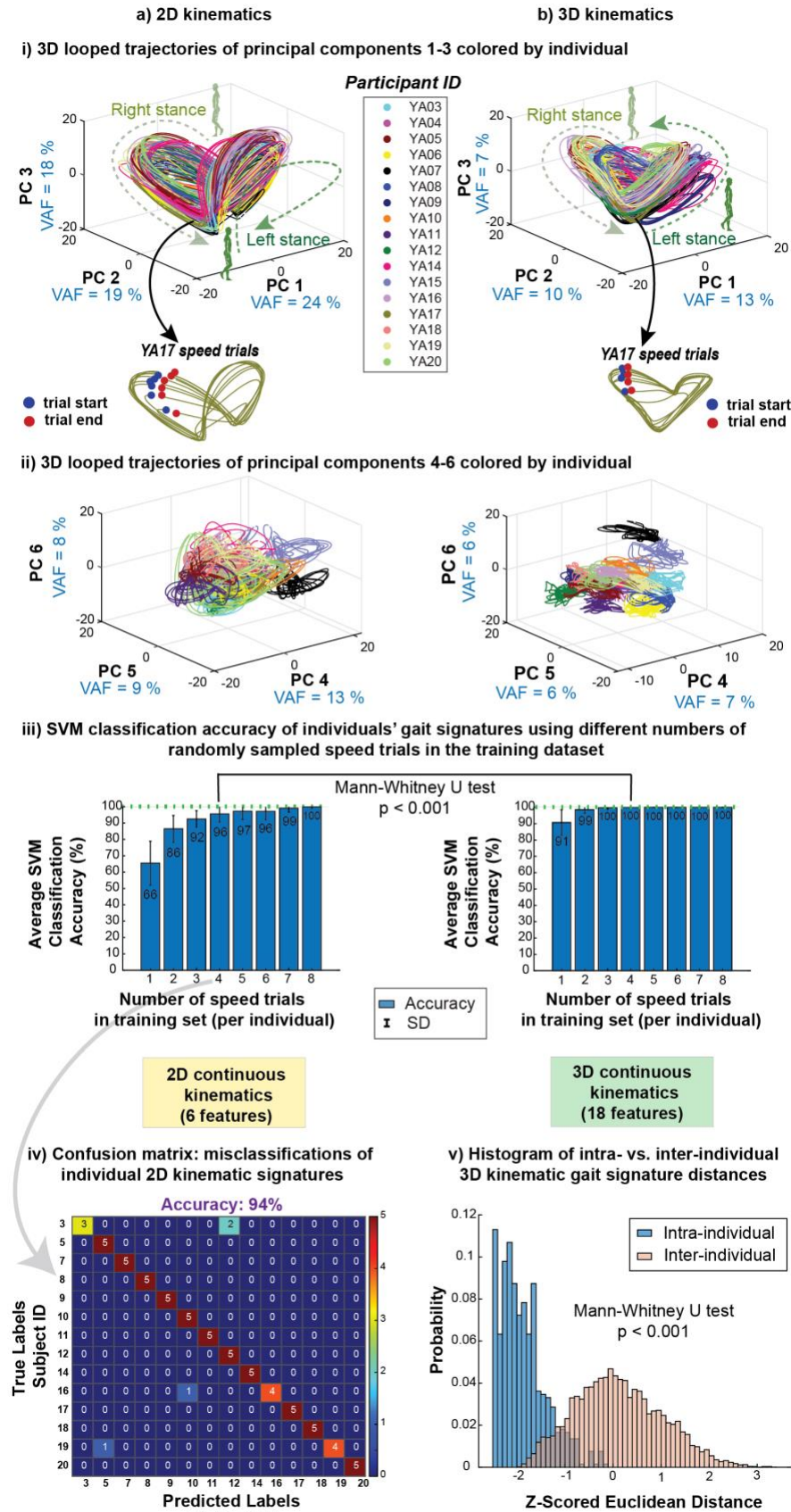
429 Phase-averaged 2D and 3D kinematic gait signatures maintain individual-specific  
430 trajectories across their entire range of walking speeds. The looped projections of the first three  
431 dominant PCs (PCs 1-3) (Fig. 5ab-i), and the second 3 dominant PCs (PCs 4-6) (Fig. 5ab-ii)  
432 belonging to each individual (specific color) cluster tightly together (Fig. 5ab-i). Higher order PCs  
433 4-6 reveal more individual specific clustering (Fig. 5ab-ii), especially in the 3D kinematic RNN  
434 signatures (Fig. 5b-ii).

435 Note that while 2D and 3D kinematic signatures were generally similarly shaped across  
436 all individuals' speed trials, 3D kinetic signatures showed 2 subsets of signatures: some  
437 participants' signatures tend more upwards in PC3 compared to other signatures (Supplementary  
438 Fig. S1a-i). Specifically, four participants (YA16, YA17, YA18 and YA19) appeared to have  
439 similarly shaped gait signatures compared to the other participants (Supplementary Fig. S1a-ii).  
440 This separation of signatures into 2 groups was not quite as evident in the combined 3D kinematic  
441 and 3D kinetic signatures (Supplementary Fig. S1b-i and ii). This division of 2 groupings of 3D  
442 kinetic signatures is more evident in the higher order PCs 4-6 (Supplementary Fig. S1a-iii) and  
443 3D MDS plots (Supplementary Fig. S1ab-iv).

444 3D kinematic signatures consistently classified individuals with significantly higher  
445 accuracy than 2D kinematic gait signatures, regardless of the number of speed trials per  
446 individuals used in the SVM training set. The classification accuracies of 2D kinematic gait  
447 signatures were significantly lower than the 3D kinematic gait signatures across one to eight  
448 speed trials in the training set ( $p \leq 0.001$ ,  $-0.27 < r > -1.01$ ). If including at least four speed trials  
449 in the training set, 3D kinematic signatures achieved almost perfect classification accuracy of  
450 99.8% (CI: 99.1-100%) (Fig. 5b-iii), whereas 2D kinematic signatures achieved 95% (CI: 88.2-  
451 100%) (Fig. 5a-iii). To attain perfect individual classification accuracy for 3D kinematic signatures  
452 (100%), a minimum of seven training speeds are required, however, even with the inclusion of  
453 additional speed trials up to eight in the training set, 2D kinematic signatures failed to reach 100%  
454 accuracy (Fig. 5a-iii). In a representative confusion matrix of a single classification iteration using

455 run of 2D kinematic signatures, we observed at least 3 instances of individual misclassification  
456 (Fig. 5a, iv). Classification analyses did not substantially improve when adding kinetic data  
457 (Supplementary Fig. S1a-v). Our analysis using 26 bilateral, discrete biomechanical variables  
458 (Supplementary Table T1) achieved  $92.2 \pm 0.1\%$  classification accuracy with only four randomly  
459 selected speed trials per individual in the SVM training set. Kinematic-only variables yielded  
460 similar high average accuracy at  $91.2 \pm 0.1\%$ . However, kinetic-only variables had significantly  
461 lower accuracy ( $p < 0.001$ ) at of  $64.3 \pm 0.2\%$ , with misclassifications up to 12 out of 14 individuals'  
462 speed trials.

463 Analysis of the inter- and intra- individual Euclidean distances between 3D kinematic  
464 signatures in 3D MDS space demonstrates that intra-individual distances are smaller than inter-  
465 individual differences ( $p < 0.001$ ), further supporting for the individual-specific nature of gait  
466 signatures within our cohort of able-bodied gait (Fig. 5b-v). The proportion of distances above two  
467 standard deviations (SD) ( $|z\text{-score}| > 2$ ) were 0% and 2.2% for intra- and inter-individual distances  
468 respectively. The proportion of distances below two SDs were 48.8% and 0% for intra- and inter-  
469 individual distances respectively.



471 **Figure 5: Kinematic gait signatures are individual-specific. i) 3D looped trajectories of the**  
472 **first 3 principal components (PCs 1-3) of a) 2D kinematic and b) 3D kinematic gait**  
473 **signatures are individual-specific across speeds. Individual's trials (same color) are**  
474 **grouped closely together with similar shapes. ii) 3D looped representations of the second**  
475 **set of principal components (PCs 4-6) reveal greater individual specific clustering in a) 2D**  
476 **kinematic signatures, and stronger differentiation observed in b) 3D kinematic signatures.**  
477 **iii) Individual classification accuracy is lower using a) 2D kinematics vs. b) 3D kinematics**  
478 **across varied number of speed trials in the classification model training set. 3D kinematic**  
479 **signatures exhibited robust classification of individuals, achieving a mean accuracy of**  
480 **99.8% (CI: 99.1% to 100%), with a minimum of four speed trials in the training set,**  
481 **surpassing the accuracy of 2D kinematics, which achieved 96% (CI: 88.2-100%). Please**  
482 **note that significant differences exist between 2D and 3D kinematic signature accuracies**  
483 **regardless of the number of speed trials in the training set. However, for clarity, we**  
484 **specifically emphasize the statistical comparison in the illustration using only four speeds**  
485 **in the training set as this is where 3D kinematic signatures attain near perfect (100%)**  
486 **classification accuracy. iv) A representative confusion matrix from a single classification**  
487 **model run shows that several individuals were misclassified when four speed trials per**  
488 **individual were included in the training set. v) The intra-individual trial distances in MDS**  
489 **space for 3D kinematic signatures are smaller than the intra-individual distances, further**  
490 **showcasing the individual-specificity across all speed trials of an individual.**

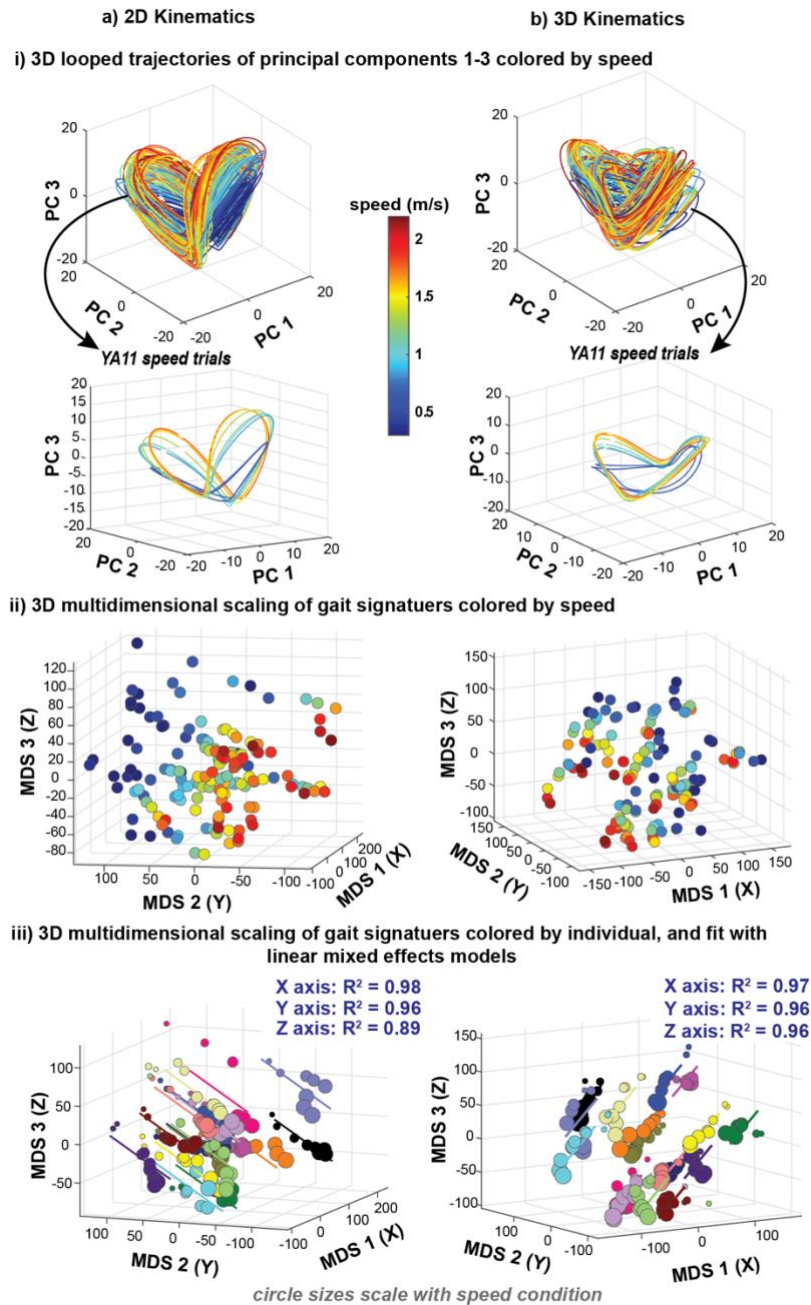
491  
492 **3.4 Gait signatures are modulated consistently with changes in walking speed**

493       Despite showing that gait signatures are individual-specific across speeds (Fig. 5), 2D and  
494 3D looped kinematic gait signatures (colored by speed) appear similar in structure and shape  
495 (Fig. 6ab-i). Both gait signature types show that slower trials (blue) are more flattened in PC3 and  
496 concentrated to the center of all speed signatures, whereas faster speeds are more expanded in  
497 PC3 and found on the outskirts of all signatures (Fig. 6ab-i, top row). This result can be seen in a  
498 representative gait signature across speeds (Fig. 6ab-i, YA11 speed trials).

499       3D gait maps of both 2D and 3D kinematic gait signatures colored by gait speed reveal  
500 that slower speeds (blue) across subjects are distinctly located in one region of the map and faster  
501 speeds (red) are in another region of the map (Fig. 6ab-ii). This modification by speed is more  
502 noticeable in 2D signatures than in the 3D signatures.

503       We found that across participants, the 3D MDS representation of gait signatures change  
504 in a similar direction with changes in gait speed (Fig. 6ab-iii). Notably, even at extremely slow  
505 speeds (0.3 m/s), similar to those observed in stroke survivors, the gait signatures maintained a  
506 consistent linear relationship with faster speeds. Linear mixed effects models accurately  
507 explained the relationship between individuals' MDS coordinate representations of their 3D  
508 kinematic gait signatures and speed with high accuracy ( $R^2 > 0.95$ ) for each coordinate (Fig. 6b-  
509 iii). However, the accuracy was lower for 2D kinematics ( $R^2 > 0.89$ ) (Fig. 6a-iii). Note that the p-  
510 value for the linear MDS coordinate fits in the Y axis of the 3D kinematic signatures were not  
511 significant ( $p = 0.28$ ).

512  
513



514

515 **Figure 6: Gait signatures hold information about walking speed.** i) 3D looped trajectories  
 516 of principal components 1-3 colored by gait speed show that similar speed trials are  
 517 shaped similarly in a) 2D kinematic and b) 3D kinematic signatures. Slower speed  
 518 signatures (blue) are concentrated in the center of all signatures and faster speed  
 519 signatures (red) on the outskirts, fanning outward and upward in PC3. ii) 3D MDS  
 520 visualizations of all signatures colored by speed illustrates that slower speeds (blue)  
 521 across individuals are in the top left region of the map for a) 2D kinematic signatures and  
 522 in the right half region of the gait map for b) 3D kinematic signatures. iii) 3D MDS  
 523 visualizations of all signatures colored by individual fit with linear mixed effects models  
 524 show that individuals gait signatures change similarly and linearly with change in gait  
 525 speed.

526 **3.5 Within individuals, 3D MDS coordinates of gait signatures vary linearly with speed**

527 Linear regression of each individual's 3D MDS gait signature coordinates separately (XYZ)  
528 showed consistently strong and significant associations between changes in the X-axis ( $R^2 > 0.50$ ;  
529  $p < 0.02$ ) across participants, but not in the Y- or Z-axes (Fig. 7a). X and Z significant slopes are  
530 negative, whereas Y has significant slopes that are positive and negative (Fig. 7b). Moreover,  
531 distinct clusters of individuals exhibited similar changes in their gait signatures with speed were  
532 evident, particularly in the X and Z coordinate slope values. These clusters were observed: a)  
533 around the mean value (red dotted line), b) above the upper limit of the 95% confidence interval  
534 (gray dotted line), and c) below the lower limit of the 95% confidence interval (Fig. 7a).

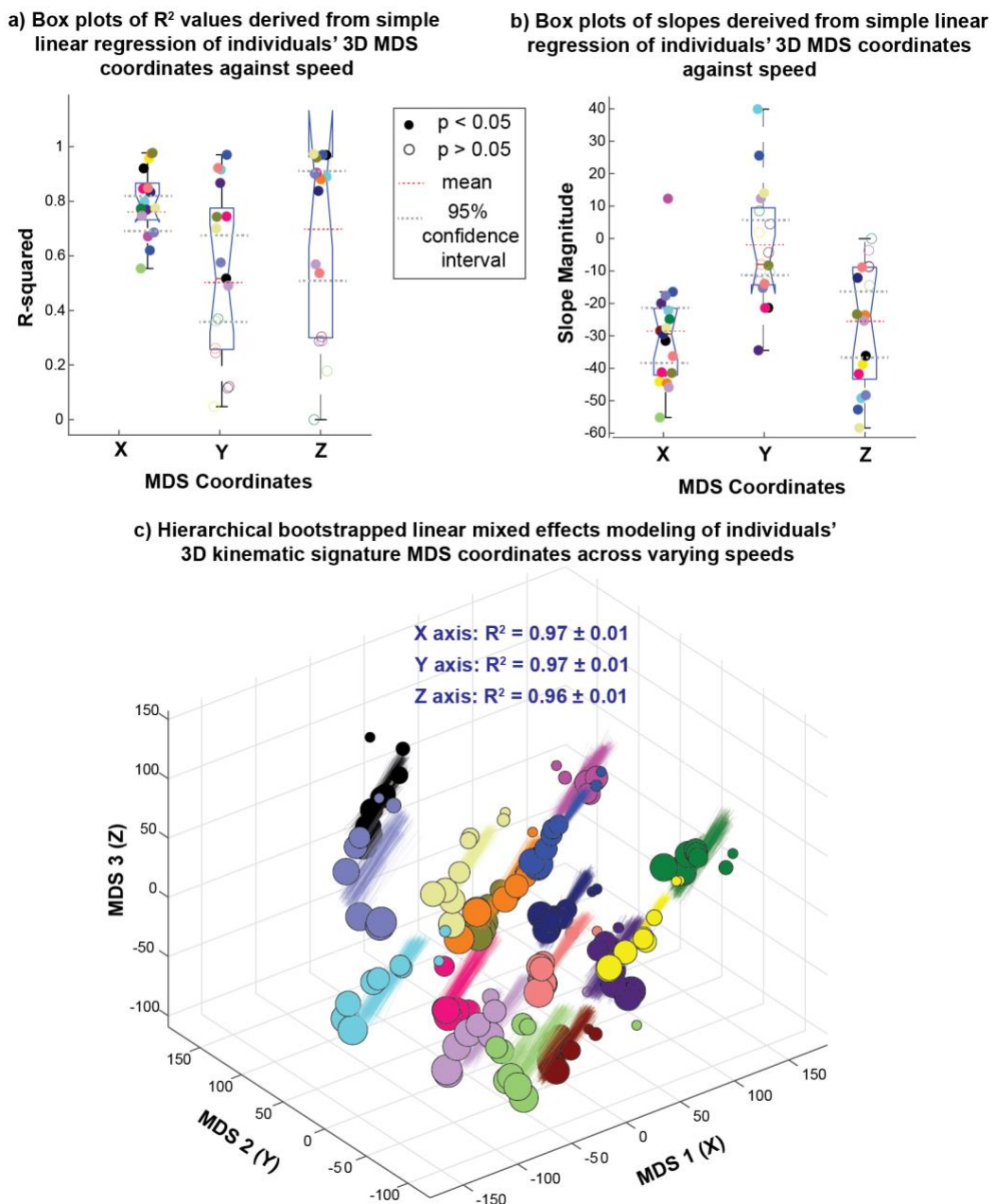
535 **3.6 Stability of linear mixed effects model parameters across individuals**

536 Linear mixed effects (LME) models tested the similarity of the linear relationships between  
537 gait signatures and speed across the entire cohort. Hierarchical bootstrapping results confirmed  
538 that robustness of the LME models to variations in input data, the number of trials per individual  
539 and speed trials used to train the model. Consequently, LME models were deemed suitable for  
540 accurately predicting the locations of 3D kinematic gait signatures with respect to speed (Fig. 7c).  
541 Note that a few Y-coordinate models resulted in non-significant p-values. The X, Y, Z sensitivity  
542 of the  $B_1$  (fixed slope) parameter was  $-0.30 \pm 0.03$ ,  $-0.02 \pm 0.02$  and  $-0.27 \pm 0.03$  respectively.  
543 The X, Y, Z sensitivity of the  $B_0$  (fixed intercept) parameter was  $37.5 \pm 5.7$ ,  $3.7 \pm 5.8$  and  $35.0 \pm$   
544  $5.5$  respectively. The standard deviation ranges of individual random intercepts for the X, Y, Z  
545 coordinates were  $[4.3 - 9.7]$ ,  $[4.2 - 8.2]$  and  $[3.9 - 6.4]$  respectively.

546 Histograms of residuals across the three LME models (representing X,Y,Z coordinate  
547 locations) exhibited normal distributions centered around zero (Supplementary Fig. S2a).  
548 Furthermore, residual vs. predicted coordinate plots show that the variance of residuals across  
549 various predictions are constant (homoscedasticity) (Supplementary Fig. S2b), meaning that the  
550 models are generally well-behaved.

551

552



553

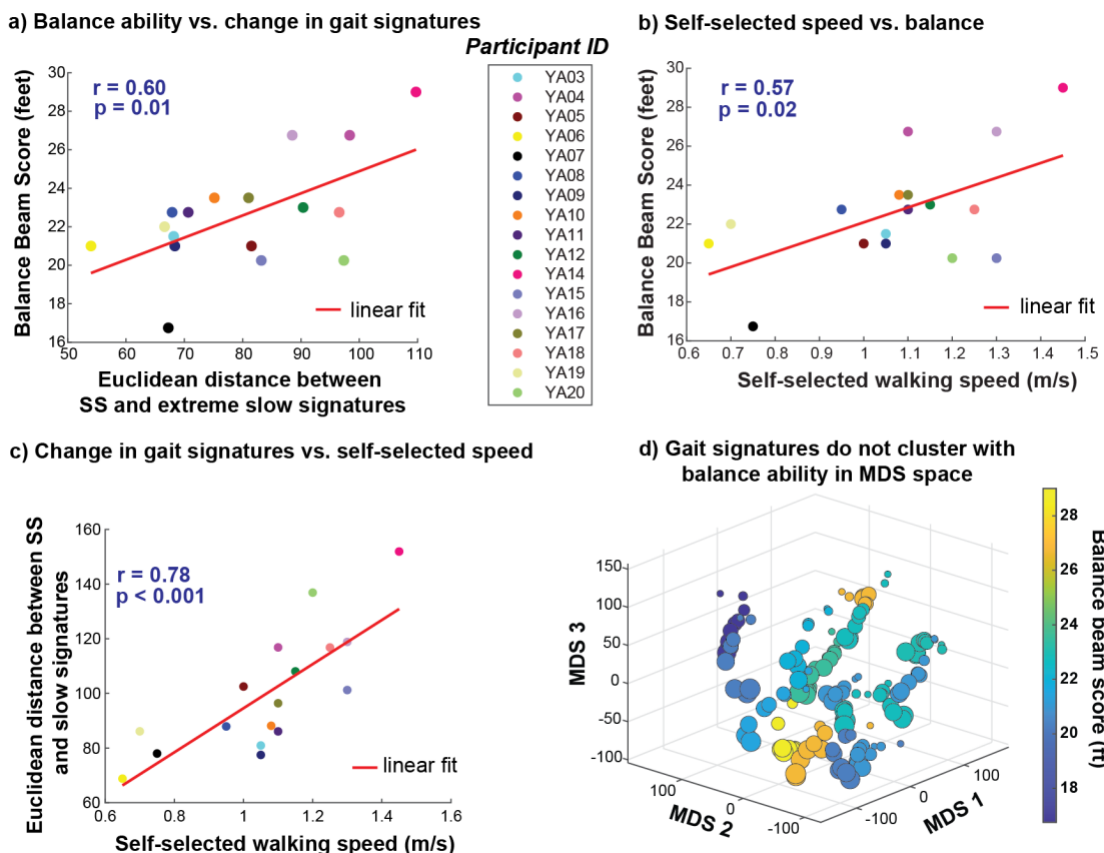
554 **Figure 7 Individual's gait signatures change linearly with speed. Simple linear regression**  
555 **of individuals' 3D MDS coordinates vs. speed show similar a)  $R^2$  values and b) slopes**  
556 **across individuals. c) Hierarchical bootstrapping of linear mixed effects shows that the**  
557 **linear relationship of MDS coordinates with speed is robust across variability in model**  
558 **input data, the number of speed trials selected per individual, and the randomness of the**  
559 **selected speed trials used in model.**

560

561

### 562 3.7 Associations between gait signature changes and balance ability

563 Walking balance ability may be associated with the extent to which individuals alter their gait  
564 signatures across speeds. We identified a moderately positive correlation between individuals' narrow-  
565 ing balance beam score and changes in gait signatures (Euclidean distance between self-  
566 selected and extremely slow speed walking gait signatures) ( $p = 0.01$ ,  $r = 0.60$ ) (Fig. 8a).  
567 Individuals with better balance (higher scores) alter their gait signatures more from SS to extreme  
568 slow. Additionally, we observed a moderate positive correlation between participants' SS speed  
569 and their performance on the narrowing balance beam (Fig. 8b), where participants' with faster  
570 SS speeds exhibited better performance compared to those with slower SS speeds ( $p = 0.02$ ,  $r = 0.57$ ). Further,  
571 individuals with slower SS speeds changed their gait signatures less between the SS and extreme slow  
572 speeds (Fig. 8c). However, changes in gait signatures between participants' SS and extreme fast  
573 speeds were not associated balance ( $p = 0.15$ ,  $r = -0.37$ ) (Supplementary Fig. S3a), or self-selected walking speed  
574 ( $p = 0.07$ ,  $r = -0.45$ ) (Supplementary Fig. S3b). In a 3D MDS map of all gait signatures, there is no discernable trend in the spatial arrangement of  
575 individuals' according to their narrowing balance beam score (where similar colors indicate similar  
576 balance scores) (Fig. 8d). For instance, the 2 groups of gait signatures colored orange are located  
577 distant from each other, and both are close to individuals with significantly lower narrowing  
578 balance beam scores (Fig. 8d).  
579



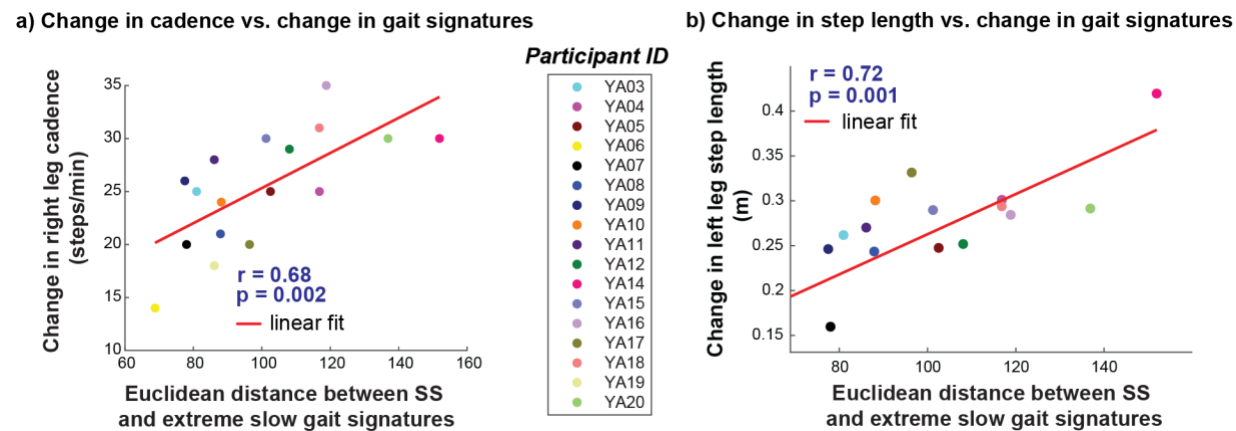
580

581 **Figure 8: Balance ability may be associated with the extent to which individuals modulate**  
582 **their gait signatures with changes in speed. a) A moderately positive linear relationship**  
583 **exists between balance ability and the change (Euclidean distance) between SS and**

584 **extreme slow speed gait signatures- individuals with better balance modulate their gait**  
585 **signatures more when reducing speed from SS to extreme slow walking speeds. b) A**  
586 **moderately positive linear relationship exists between self-selected walking speed and**  
587 **balance ability- individuals with better balance prefer walking at faster self-selected**  
588 **walking speeds. c) A strong positive linear relationship exists between change in gait**  
589 **signatures between SS and extreme slow speed and self-selected walking speed. d) 3D**  
590 **MDS representation of all individuals' gait signatures colored by their narrowing balance**  
591 **beam score reveal no clustering of signatures in this space.**

592 **3.8 Exploring associations between changes in gait signatures and discrete**  
593 **spatiotemporal variables with speed**

594 Changes in gait signatures from SS to extreme slow speeds, but not extreme fast speeds,  
595 are correlated with changes in two of five spatiotemporal biomechanical metrics (cadence, step  
596 length, swing duration, stance duration and step width). Significant correlations were identified  
597 between SS and extreme slow speed gait signatures and changes in right cadence ( $p = 0.002$ ,  $r$   
598 = 0.68) (Fig. 9a) and left step length ( $p = 0.001$ ,  $r = 0.72$ ) (Fig. 9b). However, there was no  
599 significant correlation between any of the 5 bilateral spatiotemporal variables and changes in gait  
600 signatures between SS and extremely fast walking speeds ( $p > \alpha_{\text{Bonferroni}} = 0.005$ ).



601

602 **Figure 9: A strong positive linear relationship exists between the Euclidean distance**  
603 **between self-selected and extreme slow speed signatures and changes in a) right leg**  
604 **cadence and b) left leg step length**

605 **3.9 Discrete spatiotemporal variables show strong linear relationships speed, but**  
606 **cannot distinguish between individuals**

607 Trial-averaged discrete variables also showed linear relationships with gait speed  
608 (Supplementary Fig. S4). Cadence and step length have strong, positive relationships with  
609 increasing gait speed (Supplementary Fig. S4a-i and iii), while swing duration and stance duration  
610 show strong, negative relationships with increasing speed (Supplementary Fig. S4a-ii and iv) at  
611 the Bonferroni-adjusted significance level of  $\alpha = 0.005$  for  $n = 10$  variables (all  $p$ -values  $< 0.001$ )  
612 (Supplementary Fig. S4a). The variability of these variables at the extreme slow speed (0.3m/s)  
613 showed high variability (Supplementary Fig. S4). Stance width did not demonstrate a significant  
614 correlation with speed ( $p = 0.9$ ,  $r = 0.03$ ). Spatiotemporal variables only discriminated individuals  
615 with average classification accuracy of  $55.7 \pm 0.2\%$ . A confusion matrix of a representative

616 classification run illustrates that as many as 11 out of 14 individuals were misclassified  
617 ([Supplementary Fig. S4b](#)).

## 618 **4 Discussion**

### 619 **Summary**

620 Machine-learning-based dynamic gait signatures holistically encode individual differences  
621 and systematic changes in gait dynamics with walking speed. Individual differences in gait  
622 amongst able-bodied young adults are distinguishable within a common, low-dimensional latent  
623 space of the gait dynamics model regardless of differences in how slow or fast they walk.  
624 Differences across individuals are evident using RNN models based on both 2D and 3D  
625 kinematics, suggesting that consistent gait coordination patterns within individuals can be  
626 captured from camera-based measures. In contrast, gait signatures trained using kinetics did not  
627 improve discrimination and their representations were high-dimensional, suggesting that kinetic  
628 variables do not maintain consistent coordination across speeds. Although there are unique  
629 differences between individuals' gait signatures, the changes in these signatures as speeds  
630 change are predictable, enabling us to identify a unifying linear relationship that explains how  
631 able-bodied individuals' gait signatures alters with speed. Within this common linear relationship,  
632 however, the degree to which individuals modify their gait signatures is variable and is related to  
633 their balance ability and self-selected walking speed. Overall, these insights underscore the need  
634 to identify unifying principles regarding the physiological or biomechanical factors that underpin  
635 these changes. The gait signatures approach may be useful to identify individual differences in  
636 gait across a variety of applications, notably in sports and personalized gait rehabilitation.

637 The individual-specific gait signatures discovered by our framework are consistent with  
638 the idea that individuals maintain consistent, highly characteristic gait dynamics across a variety  
639 of walking speeds<sup>[3,4,53]</sup>. Our study complements previous research by showing that individuals'  
640 gaits remain individual-specific across a wide range of speeds, rather than solely at self-selected  
641 walking speeds<sup>[1]</sup> or a more limited range of speeds<sup>[6]</sup>. Our cohort of able-bodied adults served as  
642 a rigorous test case, demonstrating the robustness of individual classification even in a healthy,  
643 young population with relatively similar dynamics. These results suggest potential discriminatory  
644 effectiveness in stroke and other patient populations as well. We show that even at very slow  
645 speeds, able-bodied gait signatures can be approximated by a linear model. Notably, prior studies  
646 have shown that walking at extremely slow speeds alter baseline gait coordination more  
647 profoundly than fast walking speeds<sup>[40,41]</sup>, and in our dataset, we observe high inter-individual  
648 variability in spatiotemporal parameters at very slow walking speeds. We thus postulate that  
649 walking at extreme slow speeds may necessitate distinct gait dynamics, given that observable  
650 differences in muscle coordination also exist at slow versus self-selected walking speed<sup>[54]</sup>. This  
651 effect could be attributed to the fact that slow walking is more akin to a postural task involving a  
652 series of weight shifts. Further, we hypothesize that there may be a greater deviation in dynamics  
653 near individuals' walk-to-run transition speed. However, our gait signatures remained individual-  
654 specific and approximately linear across the entire spectrum of walking speeds, even at extreme  
655 fast and slow speeds. Capturing the processes governing the progression of inter- and intra- limb  
656 gait variables over time offers a more comprehensive speed-independent characterization of  
657 individuals.

658 Kinematic data adequately capture individual differences in gait dynamics that differentiate  
659 individuals. Here we compared 3D kinematic signatures to the 2D kinematics approach from our

660 prior work<sup>[6]</sup>. We found a small but significant improvement in individual discrimination using 3D  
661 kinematic signatures. However, the 96% and higher average discriminatory accuracy of 2D  
662 kinematics suggests a significant amount of information can be garnered solely from motions in  
663 the sagittal plane. Improvements in the individual classification accuracy by 3D kinematic gait  
664 signatures are likely due to the added information from movement in the frontal and transverse  
665 planes. For patient populations with more frontal- and transverse-plane gait deviations<sup>[23–25]</sup>,  
666 generating gait signatures from 3D kinematic data may be more important for differentiating  
667 between individuals. Additionally, the choice between 2D and 3D kinematics affects equipment  
668 requirements, with 3D analysis often requiring multiple cameras compared to 2D analyses<sup>[55–57]</sup>.  
669 The efficacy of using 2D kinematics in gait analysis has already shown promise in conditions such  
670 as spastic tetraparesis<sup>[58]</sup>, cerebral palsy<sup>[59]</sup>, and cancer survivors<sup>[60]</sup>. Moreover, 2D kinematics-  
671 based gait signatures, such as from gait videos, may still enable characterization of gait dynamics  
672 in diverse cohorts when 3D motion capture is not feasible<sup>[61–63]</sup>.

673 We were surprised that the addition of kinetics did not improve the individual  
674 distinguishability of gait signatures. The fact that kinetic data could not be modeled in a low-  
675 dimensional space within the model suggest that the dynamics governing kinematics are sufficient  
676 to distinguish individuals across speeds compared to the dynamics of forces, which are more  
677 directly related to the biomechanical demands of maintaining dynamics underlying kinematic  
678 patterns. Considering that the recurrent neural network (RNN) learns to model the evolving  
679 neuromechanical dynamics of gait over time, it is plausible that the RNN may be able to encode  
680 similar information about an individual to what is contained in kinetic data. Moreover, previous  
681 research has used kinematic data to infer kinetic data<sup>[29,30]</sup>, suggesting that kinematics encompass  
682 information integral to kinetics. Whether kinetic data enhance classification accuracy in people  
683 with neuro-pathologies such as stroke needs more evaluation in future work. Nonetheless,  
684 eliminating the need for costly force plates in gait analysis remains advantageous.

685 Our data show that able-bodied gait signatures change predictably with speed. Despite  
686 individual-specific differences in gait signatures, we found consistent directional changes in 3D  
687 MDS representations of gait signatures with speed across participants. Similarly, many  
688 researchers have found linear relationships between simple discrete spatiotemporal variables  
689 with gait speed<sup>[14,16,17,36,37,64]</sup>. These variables, however, describe aggregated information across  
690 individuals' entire stride (e.g., peak, or averaged gait metrics). We show that changes in our gait  
691 signatures with speed are indeed moderately correlated with spatiotemporal variables such as  
692 cadence, step length, stance duration and swing duration, suggesting that our gait signatures  
693 framework holistically captures the information found in these composite variables. Furthermore,  
694 studies have shown significant relationships between gait speed and discrete kinematic<sup>[39,65–67]</sup>  
695 and kinetic variables<sup>[39,68]</sup>. However, these metrics only provide information at discrete points in  
696 the gait cycle, disregarding potentially meaningful information at other time points during the gait  
697 cycle. We showed that gait signatures classified individuals with higher average classification  
698 accuracy (~99%) than spatiotemporal variables (~56%), discrete kinematic (~91%), and discrete  
699 kinetic (~64%) variables. Given that our framework uses continuous, synchronous, multi-joint data  
700 to construct gait signatures, our current results provide further support that our approach provides  
701 a more comprehensive measure of individuals' gait coordination over time.

702 Aspects of individual differences in mobility— even in able-bodied young adults— appear to  
703 play a role in shaping individuals' gait dynamics and the ability to adjust them across speeds.  
704 First, we observed that baseline gait dynamics undergo more substantial changes with extreme

705 slow walking speeds compared to extreme fast speeds. Our results suggest that individuals with  
706 better balance may more flexibly modulate their gait dynamics from SS to extreme slow walking.  
707 Second, correlation analyses suggested that participants who preferred faster self-selected  
708 walking speeds tended to perform better on the narrowing balance beam. We infer that better  
709 balance and the extent to which individuals' modulate their gait signatures likely emerge from a  
710 common underlying construct (a confounding variable)- walking speed. Slower walking speeds  
711 are associated with worse balance and greater risk of falls, particularly among older adults and  
712 individuals with neurological impairment<sup>[69,70]</sup>. Thus, the habitual walking speed preferences  
713 observed among able-bodied young adults may be linked to their individual balance capabilities.

714 The inclusion of extremely slow speeds in our analysis is particularly relevant for  
715 comparisons between able-bodied individuals and impaired populations who may walk at very  
716 slow speeds. In our previous study<sup>[6]</sup>, we investigated both able-bodied and stroke individuals  
717 across a narrower speed range, ranging from their self-selected speeds to their comfortable fast  
718 speeds, revealing minimal overlap between the speeds of the two cohorts. The speed limitation  
719 stemmed from neuromechanical impairments and safety concerns for stroke survivors.  
720 Specifically, stroke survivors walked from 0.3m/s to 0.9 m/s, while able-bodied individuals ranged  
721 from 0.9 to 1.6m/s<sup>[6]</sup>. Thus, the incorporation of these much slower speed signatures for able-  
722 bodied young adults in our current work facilitates a more unbiased comparison of gait dynamics  
723 for impaired populations, such as stroke survivors. Conversely, the inclusion of speeds up to the  
724 walk-run transition may facilitate comparisons with cohorts comprising individuals who walk at  
725 exceptionally fast speeds, such as competitive speed walkers.

726 It is important to address some potential biases and limitations in our methodology. First,  
727 we enforced a fixed extreme slow speed of 0.3m/s across participants to ensure the speed reflects  
728 that of impaired gait speeds such as stroke survivors. This imposition may have introduced a floor  
729 effect, particularly affecting taller individuals or those with longer legs. Future studies should  
730 consider scaling speeds to leg length<sup>[71]</sup>. Additionally, we did not use a multi-session approach or  
731 have a rigorous practice session<sup>[72]</sup>. Participants may select different transition speeds given more  
732 time on the treadmill. However, given the linear regression results, we do not expect conclusions  
733 to change at slightly higher or lower transition speeds. Kinematic and kinetic variables in the  
734 frontal and rotational planes may be prone to measurement errors and greater inter-individual  
735 variability due to marker positioning, but the evaluation of within-individual changes across speeds  
736 reduces this concern in the current study<sup>[27,73-75]</sup>. To improve visualization of our data and simplify  
737 analyses, we employed 3D multi-dimensional scaling of our high dimensional gait signatures (>  
738 1000D), which may have resulted in a loss of information about relative similarity between  
739 individuals and trials. The results may have changes if a higher-dimensional representation of  
740 dissimilarity was used. Our use of support vector machine classifiers to distinguish individuals  
741 across speeds presents interpretation challenges, as the learned decision boundary may be  
742 complex and difficult to interpret, providing limited insight into the underlying relationships driving  
743 classification outcomes. Additionally, using a linear mixed effects model on a relatively small  
744 dataset raises concerns regarding the reliability of estimates for the variance components for  
745 random effects. These random effects capture variability among the individuals, potentially  
746 leading to a reduction in residual variability and an inflated perception of explained variability, thus  
747 inflating the R<sup>2</sup> values.

748 The results of our study hold significant implications for real-world applications, particularly  
749 in gait research, sports training, and gait rehabilitation. Our work can potentially aid researchers

750 with determining the minimum equipment required for constructing gait signatures capable of  
751 effectively characterizing individual differences in gait dynamics. The ability of gait signatures to  
752 reliably identify individuals walking at any gait speed may also be useful in research where  
753 biometric recognition using machine learning is important<sup>[76,77]</sup>. The finding that 3D MDS gait  
754 signatures can be reasonably predicted from a limited set of speeds may offer a valuable  
755 framework similar to velocity-based training in sports conditioning<sup>[78,79]</sup>, potentially enabling  
756 trainers to pinpoint optimal training speeds for athletes or prescribe training intensities to induce  
757 desired changes in movement quality. The linear relationship between gait signatures and  
758 speed could inform modeling and control applications, aiding the development of more efficient  
759 locomotion strategies for human-robotic systems<sup>[80]</sup>. This relationship is particularly relevant given  
760 that previous systems typically operated at speeds equivalent to or lower than a participant's  
761 comfortable overground speed<sup>[81,82]</sup>. For instance, adaptive prosthetic devices and exoskeletons  
762 could be designed to mimic an individual's natural gait patterns more closely across a range of  
763 speeds. However, while gait signatures generally change linearly with speed in able-bodied  
764 adults, this relationship may not be the case for impaired individuals, underscoring the importance  
765 of future studies in understanding individual-specific response to conditions and interventions.  
766 Moreover, individual-specific signatures hold clinical value by extending treatment monitoring and  
767 measurement beyond discrete clinical measures<sup>[83]</sup>. Gait signatures may also facilitate the design  
768 of personalized gait rehabilitation programs by leveraging insights into how individual gait  
769 characteristics predict treatment efficacy<sup>[84]</sup>. The direct association between changes in gait  
770 signatures and improvements in gait quality remains unverified. Future work should explore the  
771 relationship between gait signatures and gait quality, as well as define clinically meaningful  
772 changes. Nonetheless, more research is required to understand how impaired gait signatures  
773 change with speed, considering safety concerns and the capabilities of impaired populations. Our  
774 study opens new avenues for personalized rehabilitation interventions and enhanced sports  
775 performance through informed speed selection.

776

777

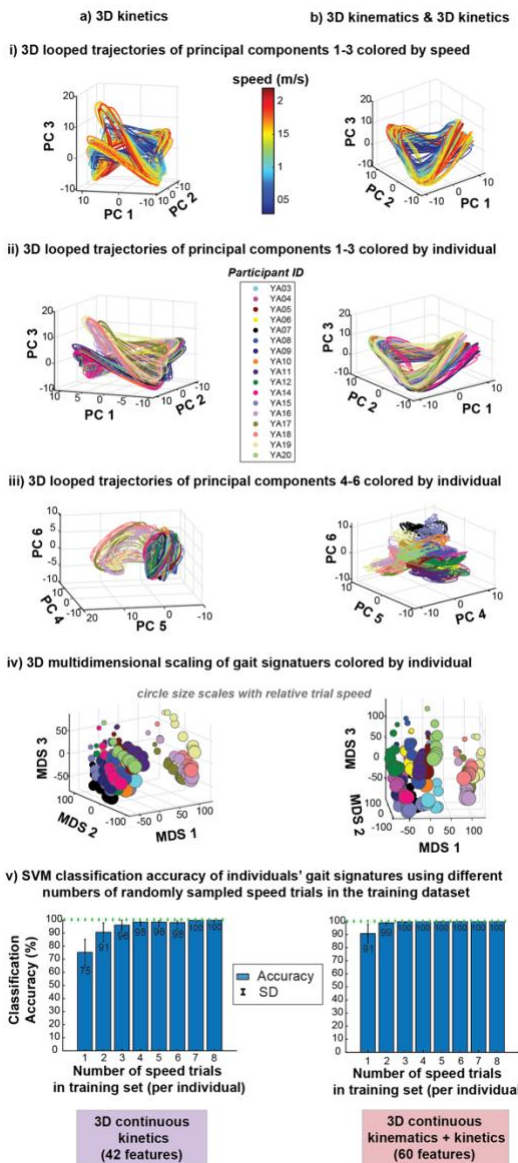
778 **5 Conclusions**

779 We used our previously developed gait signatures framework to show that gait dynamics  
780 remain individual-specific across a wide range of speeds, suggesting that this framework may be  
781 useful in characterizing individual differences in gait impairments and inform training or  
782 rehabilitation personalization. Approximately linear changes in able-bodied young adult gait  
783 signatures with gait speed allows inferences to be made about their gait dynamics at unmeasured  
784 speeds. Further, changes in gait signatures from self-selected to extreme slow speeds were  
785 correlated with balance ability, individuals' self-selected walking speed, and discrete  
786 spatiotemporal variables, pointing to specific factors that may be shaping changes in dynamics  
787 with speed. While this work focuses on solely able-bodied individuals, future work should include  
788 impaired cohorts before similar gait analyses can be translated to clinical practice. By considering  
789 the dynamic evolution of multiple gait variables over time and their modulation with speed,  
790 researchers and practitioners can gain a deeper understanding of how individuals' gait patterns  
791 adapt across different speeds. This perspective can enable the development of interventions  
792 tailored to meet the specific needs of individuals with gait impairments.

793

794

795 **6 Supplementary Figures**

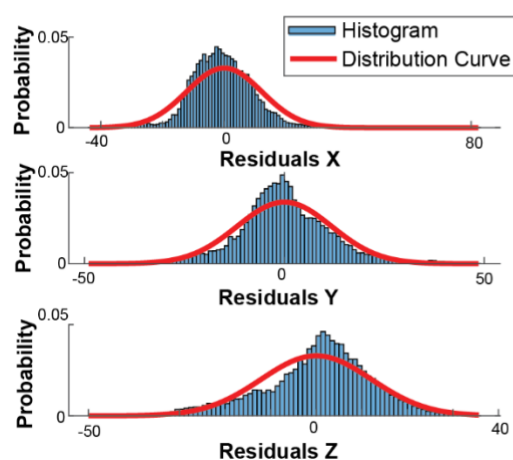


796

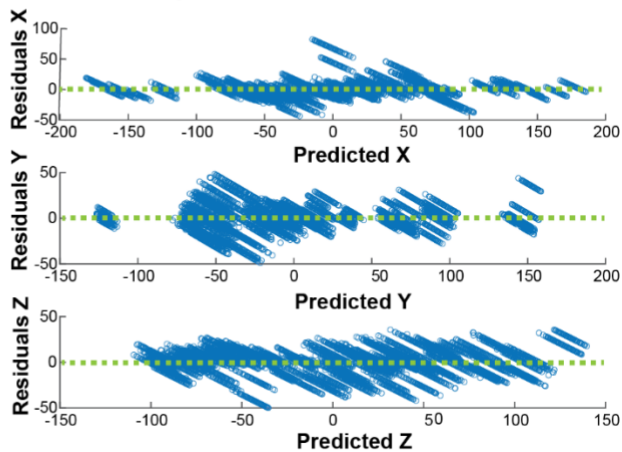
797 **Supplementary Fig. S1: Visualization of kinetic-based gait signatures a) 3D kinetics and b)**  
798 **3D kinematics & 3D kinetics. i) 3D looped trajectories of the first 3 principal components**  
799 **(PCs 1-3) of the gait signatures colored by speed shows that gait signatures at faster**  
800 **speeds (red) were more expansive than those at slower speeds (blue) ii) 3D looped**  
801 **representations of the first 3 PCs 1-3 of the gait signatures colored by individuals revealed**  
802 **that signatures are individual-specific across speeds. Kinetic signatures (a) appeared to**  
803 **form 2 groups of individuals with differing looped trajectories. iii) 3D looped**  
804 **representations of the second set of PCs 4-6 of the gait signatures colored by individual**  
805 **showcased individual-specific signatures. iv) 3D MDS visualizations of all signatures**  
806 **colored by individual further reveals a splitting of individuals into two groups. v) Individual**  
807 **classification accuracy was relatively high using a) 3D kinetics and b) 3D kinetics &**  
808 **kinematics across varied number of speed trials in the classification model training set.**

810

a) Histograms of linear mixed effect model residuals



b) Linear mixed effect model residuals vs. predicted MDS coordinate values



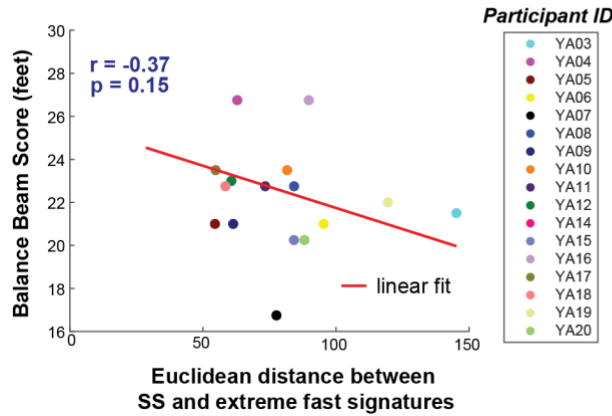
811

812 **Supplementary Fig. S2: Evaluation of LME model fits. a) Histogram of residuals across 3D**  
 813 **coordinate LME models are centered around zero. b) Residuals vs. predicted values reveal**  
 814 **homoscedasticity (fluctuation around zero) regardless of prediction value.**

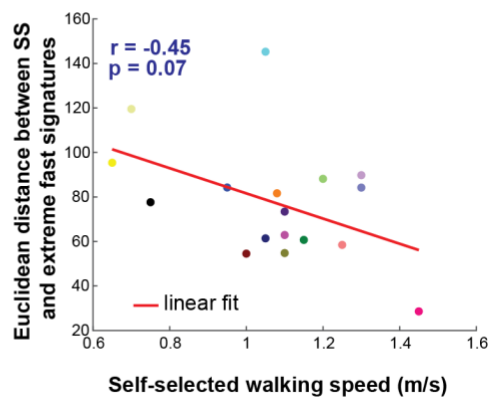
815

816

a) Balance ability vs. change in gait signatures



b) Change in gait signatures vs. self-selected speed



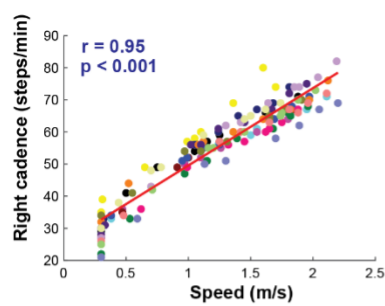
817

818 **Supplementary Fig. S3: Correlation plots showing no significant linear relationships**  
 819 **between Euclidean distance between SS and extreme fast (walk to run transition) speed**  
 820 **signatures and a) narrowing balance beam score and b) self-selected walking speed.**

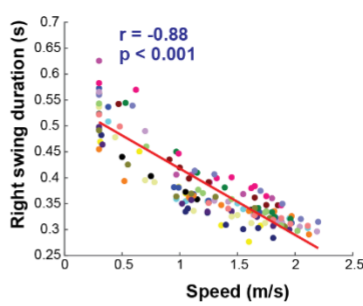
821

a) Discrete spatiotemporal variables have linear relationships with gait speed

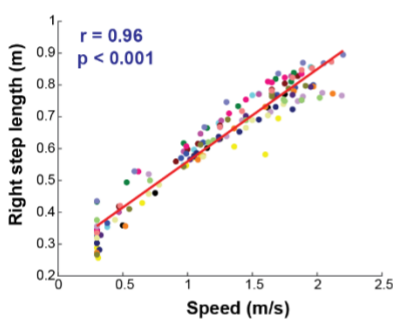
i) Cadence



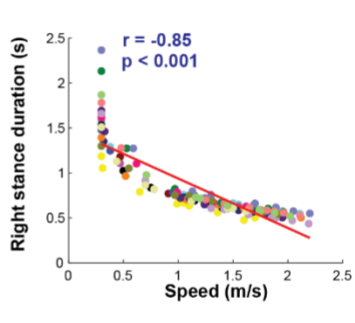
ii) Swing duration



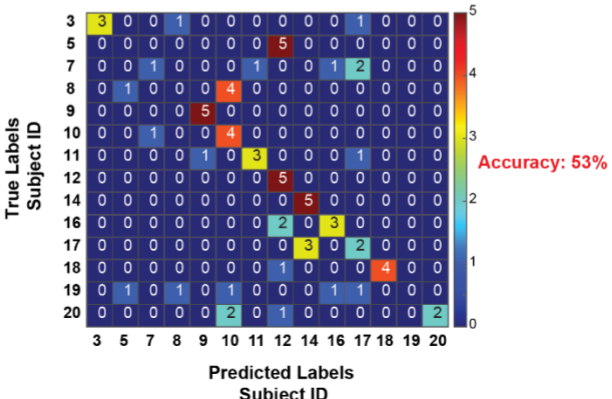
iii) Step length



iv) Stance duration



b) Confusion matrix: 5 bilateral spatiotemporal variables  
individual misclassification



822

823 **Supplementary Fig. S4: Discrete biomechanical variables show strong, linear relationships**  
824 **with speed. a) Discrete spatiotemporal variables i) cadence and iii) step length show strong**  
825 **positive linear relationships with increasing gait speed and variables ii) swing duration**  
826 **and iv) stance duration show strong negative linear relationships with increasing gait**  
827 **speed. b) Five bilateral spatiotemporal discrete variables (cadence, step length, swing**  
828 **duration, stance duration and step width) were unable to classify individuals with high**  
829 **accuracy (53%). A confusion matrix, derived from a single run of a linear support vector**  
830 **machine classification model, illustrates that multiple individuals were misclassified.**

831

832 **Supplementary Table. T1: 13 commonly used discrete biomechanical variables assessed**  
833 **bilaterally in gait analysis**

834

<b>Kinematics</b>	<b>Kinetics</b>
Step length	Peak anterior ground reaction force
Peak trailing limb angle	Push off integral
Peak hip hike	Peak ankle moment
Double support duration	Peak ankle power
Stance duration	
Swing duration	
Ankle angle at heel strike	
Ankle angle at toe off	
Knee angle at midstance	

835 **7 Data Availability Statement**

836 All data and code that support the findings in this paper has been deposited at GitHub:  
837 [https://github.com/bermanlabemory/GaitSignatures\\_HealthyYoungAdultStudy](https://github.com/bermanlabemory/GaitSignatures_HealthyYoungAdultStudy). The RNN model  
838 training and gait signature development was conducted in Python programming language. The  
839 data analysis of the generated gait signatures was conducted in MATLAB 2023a (MathWorks).  
840 The deposited materials are accessible to enhance reproducibility and advocate for open science.  
841 Additional data supporting this study's findings are available on request from the corresponding  
842 author, Taniel Winner.

843 **8 Competing Interest Statement**

844 The authors declare no competing interests.

845 **9 Funding sources**

846 TSW was supported by the Alfred P. Sloan Foundation's Minority Ph.D. (MPHD) program: G-  
847 2019-11435, NSF GRFP 1937971, and NICHD F31HD107968. MCR was supported by NICHD  
848 F32HD108927. TMK was supported by NICHD R01HD095975. TSW, MCR, and LHT were  
849 supported by the McCamish Foundation. LHT was supported by NSF CMMI 1762211 / 1761679.  
850 TSW and GJB were supported by the Simons-Emory International Consortium on Motor Control  
851 (Simons Foundation, 707102). All authors were supported by an Emory University Nexus/Synergy  
852 II Grant.

853 **10 Author contributions**

854 T.S.W, T.M.K, L.H.T, and G.J.B contributed to the conception and design of the work. T.S.W,  
855 M.C.R, and T.M.K contributed to the data collection. T.S.W. contributed to code development,  
856 analysis, generation of results and developed the initial draft of the manuscript. All authors  
857 contributed to the analysis, interpretation of the results, the writing and revision of the manuscript.

858 **11 Acknowledgements**

859 We would like to express our gratitude to Alexandra Slusarenko for her assistance with  
860 experimental data collection. We thank Benjamin Fargnoli and Jifei Xiao for their assistance with  
861 Vicon data processing. Additionally, we thank the participants who generously volunteered their  
862 time for this study.

863

864 **12 References**

- 865 1. Horst, F., Lapuschkin, S., Samek, W., Müller, K.-R. & Schöllhorn, W. I. Explaining the unique nature of  
866 individual gait patterns with deep learning. *Scientific Reports* **9**, 2391 (2019).
- 867 2. Hoitz, F., von Tscharner, V., Baltich, J. & Nigg, B. M. Individuality decoded by running patterns:  
868 Movement characteristics that determine the uniqueness of human running. *PLoS One* **16**,  
869 e0249657 (2021).
- 870 3. Schöllhorn, W. I., Nigg, B. M., Stefanyshyn, D. J. & Liu, W. Identification of individual walking  
871 patterns using time discrete and time continuous data sets. *Gait Posture* **15**, 180–186 (2002).
- 872 4. Hill, H. & Pollick, F. E. Exaggerating temporal differences enhances recognition of individuals from  
873 point light displays. *Psychol Sci* **11**, 223–228 (2000).
- 874 5. Cutting, J. E. & Kozlowski, L. T. Recognizing friends by their walk: Gait perception without familiarity  
875 cues. *Bull. Psychon. Soc.* **9**, 353–356 (1977).
- 876 6. Winner, T. S. *et al.* Discovering individual-specific gait signatures from data-driven models of  
877 neuromechanical dynamics. *PLOS Computational Biology* **19**, e1011556 (2023).
- 878 7. Williams, A. J., Peterson, D. S. & Earhart, G. M. Gait Coordination in Parkinson Disease: Effects of  
879 Step Length and Cadence Manipulations. *Gait Posture* **38**, 340–344 (2013).
- 880 8. Allen, J. L., Ting, L. H. & Kesar, T. M. Gait Rehabilitation Using Functional Electrical Stimulation  
881 Induces Changes in Ankle Muscle Coordination in Stroke Survivors: A Preliminary Study. *Front  
882 Neurol* **9**, 1127 (2018).
- 883 9. Plotnik, M., Giladi, N. & Hausdorff, J. M. A new measure for quantifying the bilateral coordination of  
884 human gait: effects of aging and Parkinson's disease. *Exp Brain Res* **181**, 561–570 (2007).
- 885 10. Plotnik, M., Bartsch, R. P., Zeev, A., Giladi, N. & Hausdorff, J. M. Effects of walking speed on  
886 asymmetry and bilateral coordination of gait. *Gait Posture* **38**, 864–869 (2013).

- 887 11. Longworth, J. A., Chlostka, S. & Foucher, K. C. Inter-joint coordination of kinematics and kinetics  
888 before and after total hip arthroplasty compared to asymptomatic subjects. *J Biomech* **72**, 180–186  
889 (2018).
- 890 12. Pau, M. *et al.* Cyclograms Reveal Alteration of Inter-Joint Coordination during Gait in People with  
891 Multiple Sclerosis Minimally Disabled. *Biomechanics* **2**, 331–341 (2022).
- 892 13. Dussault-Picard, C., Ippersiel, P., Böhm, H. & Dixon, P. C. Lower-limb joint-coordination and  
893 coordination variability during gait in children with cerebral palsy. *Clin Biomech (Bristol, Avon)* **98**,  
894 105740 (2022).
- 895 14. Fukuchi, C. A., Fukuchi, R. K. & Duarte, M. Effects of walking speed on gait biomechanics in healthy  
896 participants: a systematic review and meta-analysis. *Syst Rev* **8**, 153 (2019).
- 897 15. Kettlety, S. A., Finley, J. M., Reisman, D. S., Schweighofer, N. & Leech, K. A. Speed-dependent  
898 biomechanical changes vary across individual gait metrics post-stroke relative to neurotypical  
899 adults. 2022.04.01.486769 Preprint at <https://doi.org/10.1101/2022.04.01.486769> (2022).
- 900 16. Hebenstreit, F. *et al.* Effect of walking speed on gait sub phase durations. *Human Movement Science*  
901 **43**, 118–124 (2015).
- 902 17. Thomas, K. S., Russell, D. M., Van Lunen, B. L., Colberg, S. R. & Morrison, S. The impact of speed and  
903 time on gait dynamics. *Human Movement Science* **54**, 320–330 (2017).
- 904 18. Rosenberg, M. C. *et al.* Fastest may not maximize gait quality: differential and individual-specific  
905 immediate effects of gait speed on biomechanical variables post-stroke. 2022.12.14.22283438  
906 Preprint at <https://doi.org/10.1101/2022.12.14.22283438> (2023).
- 907 19. Tyrell, C. M., Roos, M. A., Rudolph, K. S. & Reisman, D. S. Influence of Systematic Increases in  
908 Treadmill Walking Speed on Gait Kinematics After Stroke. *Phys Ther* **91**, 392–403 (2011).
- 909 20. Browne, M. G. & Franz, J. R. The independent effects of speed and propulsive force on joint power  
910 generation in walking. *Journal of Biomechanics* **55**, 48–55 (2017).

- 911 21. Mentiplay, B. F., Banky, M., Clark, R. A., Kahn, M. B. & Williams, G. Lower limb angular velocity  
912 during walking at various speeds. *Gait & Posture* **65**, 190–196 (2018).
- 913 22. Hyodo, K., Masuda, T., Aizawa, J., Jinno, T. & Morita, S. Hip, knee, and ankle kinematics during  
914 activities of daily living: a cross-sectional study. *Braz J Phys Ther* **21**, 159–166 (2017).
- 915 23. Chen, G., Patten, C., Kothari, D. H. & Zajac, F. E. Gait differences between individuals with post-  
916 stroke hemiparesis and non-disabled controls at matched speeds. *Gait & Posture* **22**, 51–56 (2005).
- 917 24. Neckel, N. D., Blonien, N., Nichols, D. & Hidler, J. Abnormal joint torque patterns exhibited by  
918 chronic stroke subjects while walking with a prescribed physiological gait pattern. *J Neuroeng  
919 Rehabil* **5**, 19 (2008).
- 920 25. Kim, C. M. & Eng, J. J. Magnitude and pattern of 3D kinematic and kinetic gait profiles in persons  
921 with stroke: relationship to walking speed. *Gait Posture* **20**, 140–146 (2004).
- 922 26. Zajac, F. E., Neptune, R. R. & Kautz, S. A. Biomechanics and muscle coordination of human walking.  
923 Part I: introduction to concepts, power transfer, dynamics and simulations. *Gait Posture* **16**, 215–  
924 232 (2002).
- 925 27. Fiorentino, N. M. *et al.* Soft tissue artifact causes significant errors in the calculation of joint angles  
926 and range of motion at the hip. *Gait Posture* **55**, 184–190 (2017).
- 927 28. Oh, S. E., Choi, A. & Mun, J. H. Prediction of ground reaction forces during gait based on kinematics  
928 and a neural network model. *J Biomech* **46**, 2372–2380 (2013).
- 929 29. A, K. *et al.* Estimation of Ground Reaction Forces and Moments During Gait Using Only Inertial  
930 Motion Capture. *Sensors (Basel, Switzerland)* **17**, (2016).
- 931 30. Molinaro, D. D., Kang, I., Camargo, J., Gombolay, M. C. & Young, A. J. Subject-Independent,  
932 Biological Hip Moment Estimation During Multimodal Overground Ambulation Using Deep Learning.  
933 *IEEE Transactions on Medical Robotics and Bionics* **4**, 219–229 (2022).

- 934 31. Akl, A.-R., Baca, A., Richards, J. & Conceição, F. Leg and lower limb dynamic joint stiffness during  
935 different walking speeds in healthy adults. *Gait Posture* **82**, 294–300 (2020).
- 936 32. Wu, A. R., Simpson, C. S., van Asseldonk, E. H. F., van der Kooij, H. & Ijspeert, A. J. Mechanics of very  
937 slow human walking. *Sci Rep* **9**, 18079 (2019).
- 938 33. den Otter, A. R., Geurts, A. C. H., Mulder, T. & Duysens, J. Speed related changes in muscle activity  
939 from normal to very slow walking speeds. *Gait Posture* **19**, 270–278 (2004).
- 940 34. Kwon, J. W., Son, S. M. & Lee, N. K. Changes of kinematic parameters of lower extremities with gait  
941 speed: a 3D motion analysis study. *Journal of Physical Therapy Science* **27**, 477–479 (2015).
- 942 35. Goldberg, S. R. & Stanhope, S. J. Sensitivity of joint moments to changes in walking speed and body-  
943 weight-support are interdependent and vary across joints. *Journal of Biomechanics* **46**, 1176–1183  
944 (2013).
- 945 36. Kettlety, S. A., Finley, J. M., Reisman, D. S., Schweighofer, N. & Leech, K. A. Speed-dependent  
946 biomechanical changes vary across individual gait metrics post-stroke relative to neurotypical  
947 adults. *J Neuroeng Rehabil* **20**, 14 (2023).
- 948 37. Smith, A. J. J. & Lemaire, E. D. Temporal-spatial gait parameter models of very slow walking. *Gait*  
949 *Posture* **61**, 125–129 (2018).
- 950 38. Stansfield, B., Hawkins, K., Adams, S. & Bhatt, H. A mixed linear modelling characterisation of gender  
951 and speed related changes in spatiotemporal and kinematic characteristics of gait across a wide  
952 speed range in healthy adults. *Medical Engineering & Physics* **60**, 94–102 (2018).
- 953 39. Lelas, J. L., Merriman, G. J., Riley, P. O. & Kerrigan, D. C. Predicting peak kinematic and kinetic  
954 parameters from gait speed. *Gait Posture* **17**, 106–112 (2003).
- 955 40. Murakami, R. & Otaka, Y. Estimated lower speed boundary at which the walk ratio constancy is  
956 broken in healthy adults. *J Phys Ther Sci* **29**, 722–725 (2017).

- 957 41. Best, A. N. & Wu, A. R. Upper body and ankle strategies compensate for reduced lateral stability at  
958 very slow walking speeds. *Proc Biol Sci* **287**, 20201685 (2020).
- 959 42. Hreljac, A. Effects of physical characteristics on the gait transition speed during human locomotion.  
960 *Human Movement Science* **14**, 205–216 (1995).
- 961 43. Kesar, T. M. *et al.* Combined effects of fast treadmill walking and functional electrical stimulation on  
962 post-stroke gait. *Gait Posture* **33**, 309–313 (2011).
- 963 44. Kesar, T. M. *et al.* Functional electrical stimulation of ankle plantarflexor and dorsiflexor muscles:  
964 effects on poststroke gait. *Stroke* **40**, 3821–3827 (2009).
- 965 45. Kesar, T. M. *et al.* Novel patterns of functional electrical stimulation have an immediate effect on  
966 dorsiflexor muscle function during gait for people poststroke. *Phys Ther* **90**, 55–66 (2010).
- 967 46. Kesar, T. M., Binder-Macleod, S. A., Hicks, G. E. & Reisman, D. S. Minimal detectable change for gait  
968 variables collected during treadmill walking in individuals post-stroke. *Gait Posture* **33**, 314–317  
969 (2011).
- 970 47. Kingma, D. P. & Ba, J. Adam: A Method for Stochastic Optimization. Preprint at  
971 <http://arxiv.org/abs/1412.6980> (2017).
- 972 48. Revzen, S. & Guckenheimer, J. M. Estimating the phase of synchronized oscillators. *Phys. Rev. E* **78**,  
973 051907 (2008).
- 974 49. Ledesma, R. D., Valero-Mora, P. & Macbeth, G. The Scree Test and the Number of Factors: a  
975 Dynamic Graphics Approach. *The Spanish Journal of Psychology* **18**, E11 (2015).
- 976 50. Carpenter, J. & Bithell, J. Bootstrap confidence intervals: when, which, what? A practical guide for  
977 medical statisticians. *Stat Med* **19**, 1141–1164 (2000).
- 978 51. Sawers, A. & Hafner, B. Validation of the Narrowing Beam Walking Test in Lower Limb Prostheses  
979 Users. *Arch Phys Med Rehabil* **99**, 1491-1498.e1 (2018).

- 980 52. Curtin, F. & Schulz, P. Multiple correlations and bonferroni's correction. *Biological Psychiatry* **44**,  
981 775–777 (1998).
- 982 53. Troje, N. F. Decomposing biological motion: A framework for analysis and synthesis of human gait  
983 patterns. *Journal of Vision* **2**, 2 (2002).
- 984 54. Chvatal, S. A. & Ting, L. H. Voluntary and Reactive Recruitment of Locomotor Muscle Synergies  
985 during Perturbed Walking. *J Neurosci* **32**, 12237–12250 (2012).
- 986 55. Ino, T. *et al.* Validity of AI-Based Gait Analysis for Simultaneous Measurement of Bilateral Lower  
987 Limb Kinematics Using a Single Video Camera. *Sensors (Basel)* **23**, 9799 (2023).
- 988 56. Hagen, L., Kostakev, M., Pape, J. P. & Peterlein, C.-D. Are there benefits of a 2D gait analysis in the  
989 evaluation of the subtalar extra-articular screw arthroereisis? Short-term investigation in children.  
990 *Clin Biomech (Bristol, Avon)* **63**, 73–78 (2019).
- 991 57. Kidziński, Ł. *et al.* Deep neural networks enable quantitative movement analysis using single-camera  
992 videos. *Nat Commun* **11**, 4054 (2020).
- 993 58. Eliseev, A. S. *et al.* Application of 2D Gait Analysis for the Assessment of Gait Disturbance in Patients  
994 with Spastic Tetraparesis. *Sovrem Tekhnologii Med* **13**, 24–29 (2021).
- 995 59. Eek, M. N., Blomkvist, A., Olsson, K., Lindh, K. & Himmelmann, K. Objective measurement of sitting -  
996 Application in children with cerebral palsy. *Gait Posture* **96**, 210–215 (2022).
- 997 60. Beulertz, J. *et al.* Limitations in Ankle Dorsiflexion Range of Motion, Gait, and Walking Efficiency in  
998 Childhood Cancer Survivors. *Cancer Nurs* **39**, 117–124 (2016).
- 999 61. Cotton, R. J. *et al.* Optimizing Trajectories and Inverse Kinematics for Biomechanical Analysis of  
1000 Markerless Motion Capture Data. *IEEE Int Conf Rehabil Robot* **2023**, 1–6 (2023).
- 1001 62. Stenum, J. *et al.* Applications of Pose Estimation in Human Health and Performance across the  
1002 Lifespan. *Sensors (Basel)* **21**, 7315 (2021).

- 1003 63. McGuirk, T. E., Perry, E. S., Sihanath, W. B., Riazati, S. & Patten, C. Feasibility of Markerless Motion  
1004 Capture for Three-Dimensional Gait Assessment in Community Settings. *Front Hum Neurosci* **16**,  
1005 867485 (2022).
- 1006 64. Oberg, T., Karsznia, A. & Oberg, K. P. Basic gait parameters: reference data for normal subjects, 10-  
1007 79 years of age. *Journal of rehabilitation research and development* **30**, 210–223 (1993).
- 1008 65. Chung, M.-J. & Wang, M.-J. J. The change of gait parameters during walking at different percentage  
1009 of preferred walking speed for healthy adults aged 20–60 years. *Gait & Posture* **31**, 131–135 (2010).
- 1010 66. Kirtley, C., Whittle, M. W. & Jefferson, R. J. Influence of walking speed on gait parameters. *J Biomed  
1011 Eng* **7**, 282–288 (1985).
- 1012 67. Okita, Y. *et al.* The effect of walking speed on gait kinematics and kinetics after endoprosthetic knee  
1013 replacement following bone tumor resection. *Gait & Posture* **40**, 622–627 (2014).
- 1014 68. de David, A. C., Carpes, F. P. & Stefanyshyn, D. Effects of changing speed on knee and ankle joint  
1015 load during walking and running. *J Sports Sci* **33**, 391–397 (2015).
- 1016 69. Adam, C. E. *et al.* Change in gait speed and fall risk among community-dwelling older adults with  
1017 and without mild cognitive impairment: a retrospective cohort analysis. *BMC Geriatr* **23**, 328 (2023).
- 1018 70. Kelsey, J. L. *et al.* Indoor and Outdoor Falls in Older Adults are Different: The MOBILIZE Boston  
1019 Study. *J Am Geriatr Soc* **58**, 2135–2141 (2010).
- 1020 71. Hof, A. Scaling gait data to body size. *Gait & Posture - GAIT POSTURE* **4**, 222–223 (1996).
- 1021 72. Kram, R., Domingo, A. & Ferriss, D. P. Effect of Reduced Gravity on The Preferred Walk–Run  
1022 Transition Speed. *Journal of Experimental Biology* **200**, 821–826 (1997).
- 1023 73. Leboeuf, F., Barre, A., Aminian, K. & Sangeux, M. On the accuracy of the Conventional gait Model:  
1024 Distinction between marker misplacement and soft tissue artefact errors. *J Biomech* **159**, 111774  
1025 (2023).

- 1026 74. Fiorentino, N. M., Atkins, P. R., Kutschke, M. J., Foreman, K. B. & Anderson, A. E. Soft Tissue Artifact  
1027 Causes Underestimation of Hip Joint Kinematics and Kinetics in a Rigid-Body Musculoskeletal Model.  
1028 *J Biomech* **108**, 109890 (2020).
- 1029 75. D'Isidoro, F., Brockmann, C. & Ferguson, S. J. Effects of the soft tissue artefact on the hip joint  
1030 kinematics during unrestricted activities of daily living. *J Biomech* **104**, 109717 (2020).
- 1031 76. Álvarez-Aparicio, C. *et al.* Biometric recognition through gait analysis. *Sci Rep* **12**, 14530 (2022).
- 1032 77. Sepas-Moghaddam, A. & Etemad, A. Deep Gait Recognition: A Survey. *IEEE Trans Pattern Anal Mach  
1033 Intell* **45**, 264–284 (2023).
- 1034 78. Weakley, J. *et al.* Velocity-Based Training: From Theory to Application. *Strength & Conditioning  
1035 Journal* **43**, 31 (2021).
- 1036 79. Zhang, X., Feng, S., Peng, R. & Li, H. The Role of Velocity-Based Training (VBT) in Enhancing Athletic  
1037 Performance in Trained Individuals: A Meta-Analysis of Controlled Trials. *Int J Environ Res Public  
1038 Health* **19**, 9252 (2022).
- 1039 80. McCain, E. M. *et al.* Mechanics and energetics of post-stroke walking aided by a powered ankle  
1040 exoskeleton with speed-adaptive myoelectric control. *J Neuroeng Rehabil* **16**, 57 (2019).
- 1041 81. Awad, L. N. *et al.* A soft robotic exosuit improves walking in patients after stroke. *Sci Transl Med* **9**,  
1042 eaai9084 (2017).
- 1043 82. Takahashi, K. Z., Lewek, M. D. & Sawicki, G. S. A neuromechanics-based powered ankle exoskeleton  
1044 to assist walking post-stroke: a feasibility study. *Journal of NeuroEngineering and Rehabilitation* **12**,  
1045 23 (2015).
- 1046 83. Marxreiter, F. *et al.* Sensor-based gait analysis of individualized improvement during apomorphine  
1047 titration in Parkinson's disease. *J Neurol* **265**, 2656–2665 (2018).
- 1048 84. Nonnекes, J. & Nieuwboer, A. Towards Personalized Rehabilitation for Gait Impairments in  
1049 Parkinson's Disease. *Journal of Parkinson's Disease* **8**, S101–S106 (2018).

1050